

# Experimental investigations on the concrete edge failure of shear loaded anchor groups of rectangular and non-rectangular configurations

Boglárka Bokor\*, Akanshu Sharma, Jan Hofmann

*Institute of Construction Materials, University of Stuttgart, Pfaffenwaldring 4, 70569 Stuttgart, Germany*



## ARTICLE INFO

**Keywords:**

Anchorage

Anchor group

Concrete edge failure

Experimental investigation

Shear loading, test database

## ABSTRACT

The failure mode of anchorages placed close to the concrete edge and loaded in shear perpendicular towards the edge is often governed by the concrete edge breakout failure. The design provisions for concrete edge failure given in the current codes are limited in their application for anchor groups with rectangular anchor configurations only. The number of anchors in a row is limited to three for anchorages without, two for anchorages with hole clearance. Furthermore, for anchor groups with multiple anchor rows loaded in shear perpendicular and towards the edge, the failure load may be calculated by assuming the failure crack originating from the front anchor row (EN 1992-4) or from the back anchor row (fib Bulletin 58, ACI 318). The aim of this experimental study was to investigate the behaviour of shear loaded anchor groups of rectangular, triangular and hexagonal configurations undergoing concrete edge failure. A comprehensive experimental program was carried out on single anchors and anchor groups of different configurations to obtain information on (i) the group behaviour, (ii) the crack initiation and propagation, (iii) the influence of the displacement behaviour of single anchors on the behaviour of anchor groups and (iv) the influence of hole clearance pattern. The testing concept, test setup and the detailed evaluation of the test results such as load-displacement curves of the groups, load-displacement curves of single anchors, measurements on the hole clearance pattern and the investigation of the crack pattern and failure mode are discussed in this paper. Based on the evaluation of the test results presented here, a new analytical model is being developed for the concrete edge failure mode of shear loaded anchor groups that will be presented in a future paper.

## 1. Introduction and problem statement

### 1.1. General

The behaviour of anchor groups loaded in shear is rather complex due to a number of parameters, which influence the failure mode, the load distribution and the performance of the anchorage. The anchorages subjected to shear loads might fail due to anchor steel failure, concrete edge failure, prout failure or pullout failure. Which failure mode will govern, depends on the anchor type and size, steel grade, anchor embedment depth, concrete strength, edge distance, anchor configuration, anchor spacing and loading direction [1]. In the case of anchor groups placed close to a concrete edge, the failure is often governed by concrete edge breakout.

The design of single anchors according to the current codes and guidelines such as EN 1992-4 [2], fib Bulletin 58 [3] and ACI 318 [4] is relatively simple and harmonised. However, in the case of anchor groups, the provisions are limited in applicability. Only anchorages

arranged in a rectangular pattern are allowed according to EN 1992-4 and fib Bulletin 58. For anchorages without hole clearance, the maximum permissible anchor pattern is with three anchors in a row, and for anchorages with hole clearance, a maximum of only two anchors in a row is allowed. The permissible anchor configurations according to EN 1992-4 are depicted in Fig. 1. These restrictions are attributed to the semi-empirical nature of the Concrete Capacity Design (CCD) method [5], which is based on the available test data.

The existing tests on shear loaded anchorages close to the concrete edge were performed mostly on single anchors and on anchor groups of  $1 \times 2$ ,  $2 \times 1$  or  $2 \times 2$  configurations. References are included in e.g. [1,6–15], which also contain further extensive literature reviews. Note that in this paper, an  $m \times n$  configuration refers to a rectangular group with  $m$  anchor rows (one behind the other), with  $n$  anchors per row. Most of the studies focused on the load carrying capacity of the anchorage to develop an empirical formula and have defined different parameters to describe the assumed load distribution and crack pattern. Hofmann (2005) [7] performed an extensive study on anchorages

\* Corresponding author.

E-mail address: [boglarka.bokor@iwb.uni-stuttgart.de](mailto:boglarka.bokor@iwb.uni-stuttgart.de) (B. Bokor).

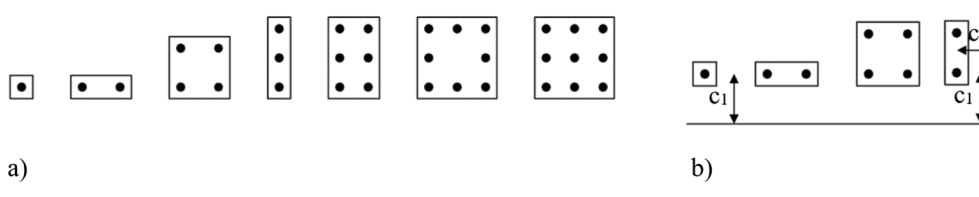


**Fig. 1.** Permissible configurations according to EN1992-4: (a) fastenings without hole clearance for all edge distances and fastenings with hole clearance situated far from edges ( $c_i \geq \max\{10h_{ef}, 60d_{nom}\}$ ) for all load directions and fastenings with hole clearance situated near to an edge ( $c_i < \max\{10h_{ef}, 60d_{nom}\}$ ) loaded in tension only; (b) fastenings with hole clearance situated near to an edge ( $c_i < \max\{10h_{ef}, 60d_{nom}\}$ ) for all load directions.

loaded in shear under arbitrary loading direction close to the concrete edge and gave recommendations for the calculation of the group resistance based on the anchor spacing to edge distance ( $s_1/c_1$ ) ratio. However, the recommendations address only anchor groups with two anchor rows arranged perpendicular to the edge. Although there are tests available on anchor groups with multiple rows, the tests were mostly carried out either far from the concrete edge or in heavily reinforced specimens or failure modes other than concrete edge breakout were governing [16–19]. Rather limited test results are available on the concrete edge failure mode of shear loaded anchor groups with more than two or three anchor rows [20–23]. Moreover, there are no regulations given for the design of anchor groups of non-rectangular configurations. According to the commentaries given in ACI 318, the CCD method is capable of extension to irregular layouts but no specific guidance is given. However, due to architectural and functional requirements, non-rectangular anchor configurations such as circular and hexagonal anchor pattern and anchorages with more than two anchor rows close to the concrete edge are also used in practice. Since no design guidelines exist for such cases, the design is based on engineering judgement.

### 1.2. Different approaches for the design of anchor groups in case of concrete edge breakout failure

The design of anchorages loaded in shear against concrete edge failure is performed according to the CCD method, which involves calculation of the basic concrete edge breakout resistance of a single anchor not influenced by other factors, and then modifying it to account for the presence of neighbouring anchors (group effect), member thickness, vicinity of the perpendicular edge, loading direction and load eccentricity as and when applicable [1–4]. In the case of anchor groups with only one anchor row (anchors placed parallel to the edge), the design provisions given in various standards are, in principle, unified since the failure crack appears from the location of the anchor row.

However, in case of anchor groups with multiple anchor rows, the failure load corresponding to the concrete edge failure may be calculated either by assuming the failure crack originating from the front anchor row (approach given in EN 1992–4) or by assuming the failure crack originating from the front, middle or back anchor row (approach followed by fib Bulletin 58, ACI 318). However, if the failure crack is considered to appear from the back or mid anchor row, only the anchors not located in the theoretical breakout body can be considered to resist shear loads for the verification for steel failure (Fig. 2). The approach to consider the failure crack originating from the first anchor row was included in EN 1992-4 because in many cases it is not obvious whether the redistribution of the shear load to the back anchor row can take place after the crack (if any) has formed at the front anchor row. This approach is deemed conservative for anchorages with multiple anchor rows since the force redistribution to the back anchor rows is completely neglected (see e.g. in [20,22,23]). If the failure crack is assumed to initiate from the back anchor row, then due to the larger edge distance, the calculated failure load is significantly higher than the failure load obtained by assuming the failure crack originating from the front anchor row. Fig. 2 highlights that according to the current rules, if

the failure crack is assumed from the front anchor row, the design is resulting in the same failure load for a group having a single anchor row or multiple anchor rows if the edge distance for the first anchor row and all other installation parameters are the same.

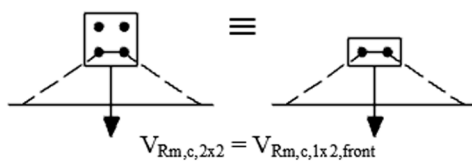
In the case of anchor groups with welded headed studs, it is evident that the anchorage is to be considered as an anchor group without hole clearance, and consequently, it can be placed at any edge distance with up to a 3 × 3 anchor pattern (compare Fig. 1). In this case, all anchors are assumed to resist shear forces, initially equally. In the case of post-installed anchors, the anchorage may be designed with or without hole clearance, which the designer should decide based on the application. However, the permissible configurations for the cases with hole clearance are limited to 2 × 2 pattern.

The experiments on anchorages with multiple rows by Grosser (2012) were performed on groups of bonded anchors with a single anchor row perpendicular to the edge having 2, 3 and 5 anchors in the row (2 × 1, 3 × 1 and 5 × 1 configurations), and loaded in shear perpendicular to the edge [20]. The behaviour of anchor groups, which failed due to concrete edge breakout, with different spacing to front row edge distance ratios ( $s_{1,1}/c_{1,1}$ ) was investigated. Grosser summarised that for anchor groups without hole clearance, the crack formation at the front anchor may be neglected for the ultimate limit state (ULS) verification, and the failure load can be taken as the failure load of the back row; however, the performance of the group should be checked for the serviceability limit state (SLS) verification. In the case of tests with hole clearance, he focused on the displacement at the failure of the corresponding single anchor to the hole clearance ratio. He reported that if the activation of the back anchor is possible before the failure of the front anchor occurs, then the shear load can be redistributed to the back anchor and the anchors are loaded equally. His approach, to not only focus on the failure loads, but also on the displacement behaviour of the different anchor rows is deemed appropriate, and concurrently highlights the importance of the evaluation of the complete load-displacement behaviour of anchorages. However, to presume whether a crack at the front anchor row will form or not, he evaluated the resistance of the front row compared to the resistance of the back row for the corresponding  $s_{1,1}/c_{1,1}$  (anchor spacing in the loading direction to edge distance of the front anchor) ratios.

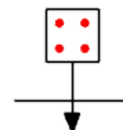
The tests by Sharma et al. [22,23] were carried out on anchor groups with headed studs welded on the embedded base plate. Groups of 1 × 2, 2 × 2, 2 × 4 and 4 × 2 configurations were investigated. It was found that the number of anchor rows influences the failure load, whereas the number of anchors per anchor row increases the stiffness of the anchorage. Furthermore, in all investigated cases, the failure crack originated from the back anchor row, which explains the higher failure loads by increasing the number of anchor rows. The findings obtained from this research call for further research on multiple anchor rows and highlight the conservatism of the current design provisions. Note that in [22], reference tests on single anchors for the corresponding anchor rows were not carried out, so the anchor group performance cannot directly be compared with the single anchor performance.

**EN 1992-4**

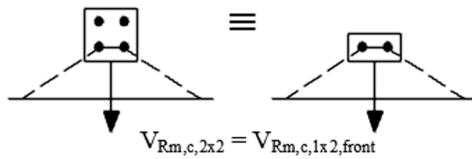
- Crack initiation considered from front row  
Concrete edge failure



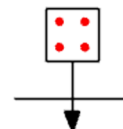
Steel failure - both anchor rows resist

**fib Bulletin 58**

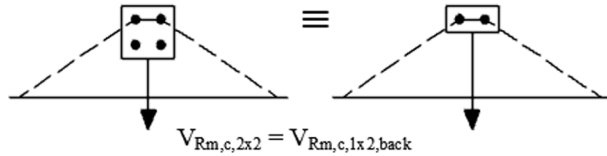
- Crack initiation considered from front row  
Concrete edge failure



Steel failure - both anchor rows resist



- Crack initiation considered from back row  
Concrete edge failure



Steel failure - only back anchor row resists

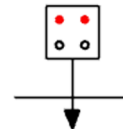


**Fig. 2.** Crack initiation and concrete edge failure in case of two anchor rows considered according to EN 1992-4 and fib Bulletin 58.

### 1.3. Objectives

Although significant research has been performed on the load-bearing behaviour of shear loaded anchorages, most of them have focused on the resistance of the anchorage to develop an empirical formula, and have defined different parameter ratios to assume the load distribution and crack pattern. With this, the behaviour of anchor groups up to  $2 \times 2$  configurations can be covered relatively accurately, still, there is no consensus among the codes and standards regarding the assumption of the failure crack. However, if anchor groups bigger than  $2 \times 2$ , or anchor groups of non-rectangular configurations shall be designed or evaluated, the load-displacement behaviour of the individual anchors and the load-displacement behaviour of the group should be checked because of the complexity of the behaviour of shear loaded anchorages.

Therefore, this study aims to extend the database on the behaviour of anchor groups loaded in shear towards the free concrete edge and failing due to concrete edge breakout. Experimental investigations were carried out on anchor groups of rectangular ( $2 \times 1$  and  $3 \times 1$ ) and non-rectangular (triangular and hexagonal) configurations in concrete specimens without the influence of member thickness and reinforcement. The tests were evaluated in order to obtain information on (i) the group behaviour of anchorages, (ii) the crack origination in case of anchor groups, (iii) the influence of the displacement behaviour of single anchors on the behaviour of anchor groups and (iv) the influence of hole clearance pattern in the base plate. However, the major aim of the conducted test program and the evaluation of experimental results is to provide the information required for the development of a relatively general analytical model for calculating the resistance of anchor groups in case of concrete edge breakout failure mode. The model should be able to predict the resistance and overall behaviour of rectangular as

well as non-rectangular anchor groups considering various geometric aspects, loading and boundary conditions. Therefore, the evaluation discussed in this paper focuses significantly on the load-displacement behaviour of anchor groups and on the load-displacement behaviour of single anchors with the corresponding edge distance.

Based on the detailed evaluation of the test results and further numerical investigations (which is beyond the scope of this paper), a general model is being currently developed, which is able to predict the performance of shear loaded anchor groups under concrete edge failure. The model will be presented in a future paper.

## 2. Experimental investigations

### 2.1. The focus of the experimental program

The experimental program presented in this paper focuses on the concrete edge failure mode of anchor groups loaded in shear perpendicular towards the free concrete edge. In addition to the group tests, reference tests on single anchors were carried out with the same parameters, such as edge distance, anchor diameter and embedment depth to enable a direct comparison with the group results. The experiments were carried out with hole clearance, and the actual gap between the anchor rod and base plate was measured prior to testing.

The experiments aimed to provide information about the load-displacement behaviour of anchor groups and single anchors with different edge distances and to highlight that the group behaviour, as well as the load distribution and redistribution, are strongly dependent on the displacement behaviour of the individual anchors of the corresponding anchor rows. Furthermore, it was aimed to show that although the first cracking can limit the design in SLS, the failure crack originates from the back anchor row. Whether the forces can be

**Table 1**

Test program on single anchors and anchor groups to investigate the influence of anchor rows on the load-displacement behaviour of shear loaded anchorages in case of concrete edge failure.

Test series ID <sup>a)b)c)d)</sup>	Test type	Edge distance of the corresponding anchor row			Anchor spacing		Edge distance of recess or breakout body	No. of tests	Remarks
		$c_{1,1}$	$c_{1,2}$	$c_{1,3}$	$s_{1,1}$	$s_{1,2}$			
		[mm]	[mm]	[mm]	[mm]	[mm]	[mm]	[-]	[-]
SS-80		80	–	–	–	–	–	3	Reference
SS-160		160	–	–	–	–	–	3	Reference
SS-240		240	–	–	–	–	–	3	Reference
GS-3×1-80-80		80	160	240	80	80	–	3	Group
GS-2×2-1-80-80		80	160	–	80	80	–	3	Group
GS-2×1-160-80		160	240	–	80	80	–	2	Group
SS-160-r80		160	–	–	–	–	80	4	With recess
SS-240-r160		240	–	–	–	–	160	4	With recess
SS-240-a(SS-160)		240	–	–	–	–	160	1	With pre-breakout formed by a single anchor of series SS-160
SS-240-a(SS-160-r80)		240	–	–	–	–	–	2	With pre-breakout formed by a group of series SS-160-r80
SS-240-a(GS-2×1-80-80)		240	–	–	–	–	–	2	With pre-breakout formed by a group of series GS-2×1-80-80

<sup>a)</sup> Nomenclature for tests on single anchors: Single Shear - tested edge distance  $c_1$  in mm.

<sup>b)</sup> Nomenclature for tests on anchor groups: Group Shear - configuration - edge distance of front anchor  $c_{1,1}$  in mm – spacing  $s_1$  in mm.

<sup>c)</sup> Nomenclature for tests on single anchors with recess: Single Shear - tested edge distance  $c_1$  in mm -  $c_1$  of recess in mm.

<sup>d)</sup> Nomenclature for tests on single anchors with pre-breakout: Single Shear - tested edge distance  $c_1$  in mm - after failure of (test series).

distributed further after the first cracking, depends on the displacement behaviour of the individual anchors and on the clearance hole pattern. Finally, the results obtained from the experimental investigations were compared to calculations based on the EN 1992-4 and fib Bulletin 58.

## 2.2. Program overview

The entire test program can be divided into two categories, 1 test program to investigate the influence of anchor rows and (2) test program on non-rectangular anchorages.

Table 1 includes the details of the first test program on single anchors and anchor groups with a line of anchors arranged perpendicular to the edge loaded perpendicular towards the edge. These investigations aimed to understand the relation between the load-displacement behaviour of single anchors with a particular edge distance ( $c_1$ ) and an  $i^{\text{th}}$  anchor of an anchor group with the same edge distance ( $c_1$ ). In the case of the anchor groups,  $2 \times 1$  and  $3 \times 1$  anchor configurations were tested (see Fig. 3 and Table 1). The edge distance for the first, second and third anchor row is represented as  $c_{1,1}$ ,  $c_{1,2}$  and  $c_{1,3}$ , respectively in Table 1. In addition, reference tests on single anchors were carried out for the individual edge distances of the anchors in the group to enable the evaluation of group behaviour based on the individual anchor load-displacement behaviour. In this test series, only one anchor per anchor row was installed to focus on the force redistribution from row-to-row.

Furthermore, in order to better understand the behaviour of anchorages undergoing concrete edge failure, two special kinds of tests were also performed:

- Shear loading tests on single anchors to investigate the influence of a “missing” concrete breakout body (of an anchor with an edge distance of  $c_{1,1}$  or  $c_{1,2}$ ). For this reason, special concrete specimens with a recess in front of the investigated anchor row were cast. The shape of the recess corresponded to the theoretical concrete breakout body of a single anchor with an edge distance of  $c_{1,1} = 80$  mm (Fig. 5b) and  $c_{1,1} = 160$  mm (Fig. 5c).
- Shear loading tests on single anchors with an edge distance of  $c_1 = 240$  mm, which were installed after the concrete edge failure of the anchor installed with  $c_1 = 160$  mm, and after removal of the breakout body. (Note: Similar investigations were carried out by Unterweger et al. [9], where the residual capacity of the back anchor was checked.) This case should simulate an anchor group, where the back anchor row can still resist forces after the front row has already completely failed. However, such a situation is very unlikely in practice, where the second anchor row is only activated when the anchor in the first row has zero resistance ( $V = 0$  kN) and no concrete is present. The amount of the redistribution in case of groups, if any, depends on the load-displacement behaviour of the anchors. In general, even after the first anchor row has reached its

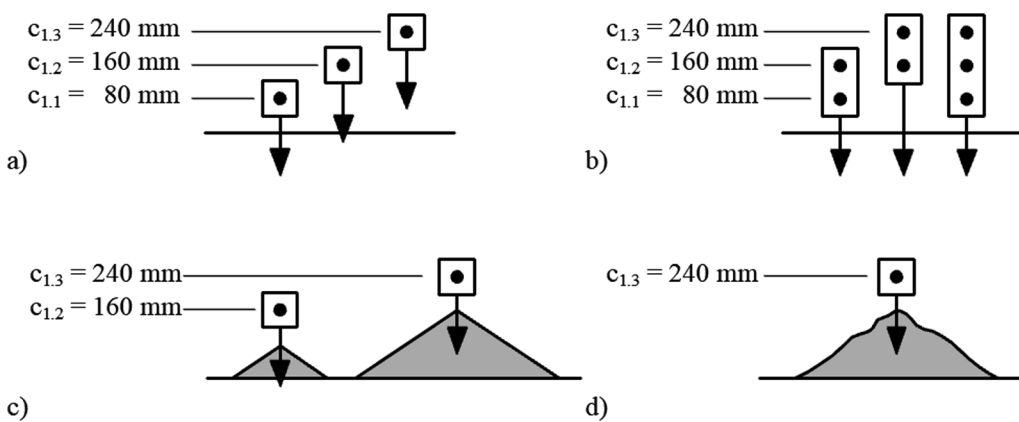


**Fig. 3.** Description of the first test program on (a) single anchors, (b) anchor groups with a line of anchors, (c) single anchors with concrete recess in the front, and (d) single anchors with pre-breakout body in the front.

ultimate load, it still contributes to the group capacity as the resistance drops only gradually due to the quasi-brittle behaviour of concrete. However, the resistance beyond peak can be considered only by taking into account the complete load-displacement behaviour of the anchor.

Thus the first test program as described in Fig. 3, consisted of tests on (a) single anchors, (b) anchor groups with a line of anchors, (c) single anchors with concrete recess in the front, and (d) single anchors with pre-breakout body in the front. The anchor size M20 ( $d = 20$  mm) and the effective embedment depth  $h_{ef} = 120$  mm were kept constant in all tests. The mean cubic compressive strength of concrete was obtained as  $f_{cc} = 31.0$  MPa. In general, 3 tests per series were performed. However, due to practical reasons, this could not be maintained in each case.

Table 2 contains the details of the second test program on anchorages with triangular and hexagonal anchor pattern, which are beyond the scope of the current regulations of EN 1992-4 and fib Bulletin 58. For better evaluation of the test results, reference tests on single anchors with corresponding edge distances were also performed. The experiments were carried out on anchorages in non-cracked concrete, which were placed close to the concrete edge with random hole clearance and were loaded perpendicular to the concrete edge. The anchor pattern of the base plates enabled for both the triangular and hexagonal groups to investigate two different test configurations by rotating the base plate by 180° for the triangular pattern and by 90° for the hexagonal pattern. However, the edge distance  $c_{1,back}$  of the back anchor row was kept constant ( $c_{1,back} = 240$  mm) for all cases (see Fig. 4). Again, the anchor diameter and anchor embedment depth were maintained as 20 mm and 120 mm respectively for all the tests.

### 2.3. Test specimens

The shear loading tests were carried out in concrete specimens of size  $163.5 \times 163.5 \times 50$  cm<sup>3</sup>, which were provided with sufficient amount of edge reinforcement to avoid the flexural failure of the specimen while applying the shear load perpendicular to the concrete edge (Fig. 5a). Special concrete specimens were cast for test series SS-160-r80 and SS-240-r160 with a recess in front of the investigated anchor row. The shape of the recess corresponded to the theoretical concrete breakout body of a single anchor with an embedment depth of  $h_{ef} = 120$  mm, edge distance of  $c_1 = 80$  mm for test series SS-160-r80 (Fig. 5b) and  $c_1 = 160$  mm for test series SS-240-r160 (Fig. 5c), respectively. It was assumed that the failure breakout body develops from the anchor tip and propagates towards the concrete edge to a depth of  $1.5c_1$ . The width of the concrete breakout body at the front edge was assumed as  $3c_1$ . The edge distances of the investigated single anchors

were  $c_1 = 160$  mm and  $c_1 = 240$  mm. Fig. 5d depicts the schematics of the test specimen with removed concrete breakout body of a prior test, which was used for the test series SS-240-a(SS-160), SS-240-a(SS-160-r80) and SS-240-a(GS-2 × 1-80-80).

The formation of the full size concrete edge breakout bodies, without the influence of neighbouring anchor groups or the reinforcement, was ensured in all tests. Sufficiently large clear distance was maintained between the outermost anchors of the groups tested in one concrete specimen, and the support distance measured from the outermost anchor of the group was  $2c_{1,back}$  on both sides (see Fig. 6).

The concrete mix was designed according to DIN EN 206 [24], with a maximum grain size of 16 mm using round gravel aggregates. The compressive strength was measured according to DIN EN 12390-15 [25] on concrete cubes with a side length of 150 mm. The concrete compressive strength of the corresponding test series is given in Section 2.2.

### 2.4. Tested anchors and installation

Epoxy-based adhesive anchor system from the company fischer (FIS EM Plus) was chosen for the experiments because of its flexible installation parameters and relatively high stiffness. The mean bond strength of the used adhesive was approximately  $\tau = 30$  N/mm<sup>2</sup>. M20 ( $d = 20$  mm) steel threaded rods of grade 12.9 ( $f_{u,nom} = 1200$  N/mm<sup>2</sup>) were used as steel element. The effective embedment depth of the anchors was  $h_{ef} = 120$  mm in all tests, which corresponds to a  $h_{ef}/d$  ratio of 6.0. The installation parameters were designed to ensure concrete edge breakout failure.

The anchors were installed according to the corresponding Manufacturer's Installation Instructions (ETA-10/0012 [26]). Holes were drilled by hammer drilling perpendicular to the concrete surface using steel templates with pilot-holes to ensure that the anchors within the group are positioned accurately and to provide an accurate edge distance. Then, the holes were cleaned using compressed air and steel brush, and the mortar was injected into the holes and the base plate was positioned on the anchors, respectively. A plastic sheet was placed between the base plate and concrete to avoid that the remaining epoxy on the concrete surface is glued to the base plate. After the prescribed curing time of the epoxy mortar, the base plate was removed and a 1.5 mm Teflon sheet was placed between the base plate and the concrete surface to minimize friction during the tests. To ensure the same initial installation conditions for the anchors, the nut was only hand-tightened and no installation torque was applied on the anchors. The annular gaps between the holes in the base plate and anchor rods were not filled, so the anchorages are to be considered as anchor groups with hole clearance.

**Table 2**

Test program for anchor groups of non-rectangular configuration.

Test series ID a) b)	Test type	Mean concrete cube compressive strength $f_{cc}$ [N/mm <sup>2</sup> ]	Edge distance of the corresponding anchor row				Anchor spacing in the loading direction $s_1$ [mm]	Anchor spacing perpendicular to the loading direction $s_2$ [mm]	No. of tests
			$c_{1,1}$ [mm]	$c_{1,2}$ [mm]	$c_{1,3}$ [mm]	$c_{1,4}$ [mm]			
SS-100		25.2	100	—	—	—	—	—	3
SS-120		27.6	120	—	—	—	—	—	3
SS-170		25.2	170	—	—	—	—	—	3
SS-200		25.2	200	—	—	—	—	—	2
SS-240b		27.6	240	—	—	—	—	—	2
GS-TRI-A		25.2	120	240	—	—	120	139	3
GS-TRI-B		25.2	120	240	—	—	120	139	3
GS-HEX-A		25.2	101	171	240	—	69.25/69.25	80/160/80	3
GS-HEX-B		25.2	80	120	200	240	40/80/40	0/138.5/138.5/0	3

a) Nomenclature for tests on single anchors: Single Shear -  $c_1$  in mm

b) Nomenclature for tests on anchor groups: Group Shear – configuration

## 2.5. Test setup

Fig. 6 shows a schematic drawing of the test setup used for anchor groups loaded perpendicular in shear towards the concrete edge. The tests were performed using rotation unrestrained load application, without using uplift restraint for the base plate. The same test setup was used for the reference single anchor tests using the corresponding loading fixture. Note that the experiments were performed with hole clearance between the base plate and the anchor rod. The diameter of clearance hole corresponded to the requirements given in EN 1992-4, Table 6.1,  $a_{cl} = 22$  mm for nominal anchor diameter of  $d_{nom} = 20$  mm. The actual annular gap was measured prior to testing. For practical reasons, the measurement was carried out from the top of the base plate. Consequently, a minor misalignment of the anchor rod might slightly falsify the measurement.

The test setup consisted of the following major components: (i) steel

supports with an adequate distance to allow the formation of an unrestricted concrete edge breakout body, (ii) slab tie-down to avoid the uplifting of the specimen, (iii) a hydraulic cylinder and high strength threaded rod for load application, (iv) a hinge to allow the free rotation of the base plate, (v) a calibrated load cell, (vi) displacement transducers for measuring the base plate displacement, (vii) a Teflon layer to minimize friction between base plate and concrete surface and (viii) a data acquisition system with computer interface.

The shear load was applied to the anchors through the base plate. The load was actuated using the 400 kN hydraulic test cylinder. To transfer the load from the hydraulic cylinder into the base plate, a high strength M24 threaded rod was used with a hinge (hinge capacity up to 120 kN) built in to the force flow to allow the possible rotation of the base plate. A calibrated load cell (20–200 kN) was used to measure the shear load applied on the anchorage. The horizontal displacement was measured using two displacement transducers (LVDT with a measuring

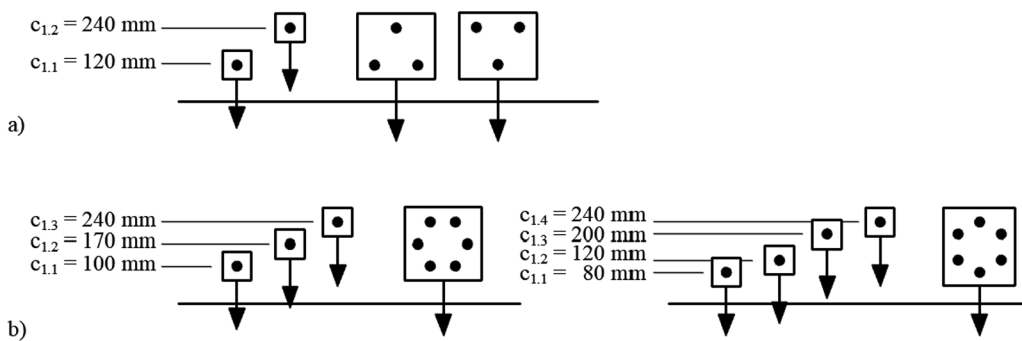
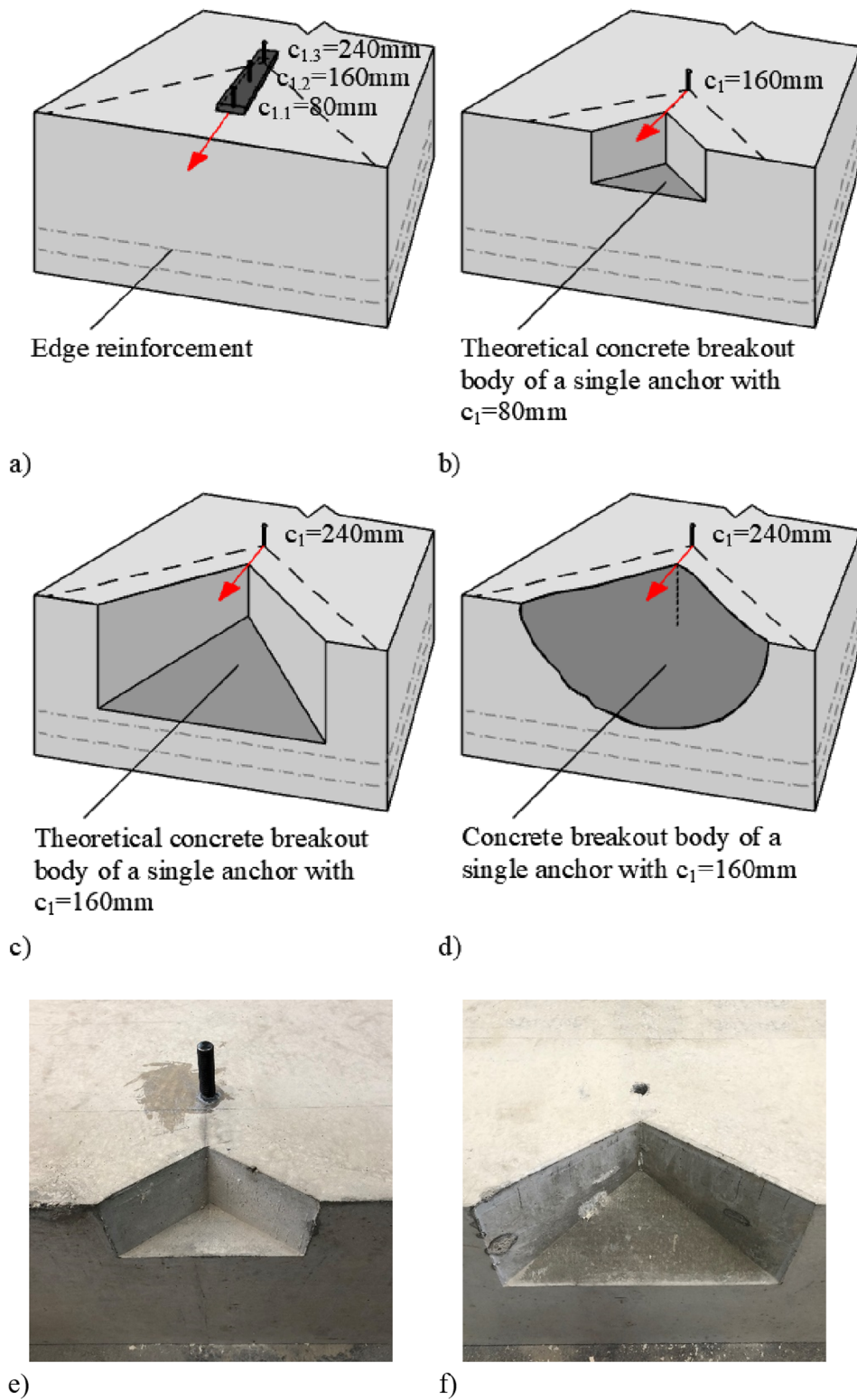


Fig. 4. Description of the second test program: Anchorages loaded perpendicular to the free edge with the corresponding reference single anchor tests (a) anchorage with a triangular pattern; (b) anchorages with hexahedral pattern.



**Fig. 5.** Schematic drawings of the test specimen (a) for single anchor and group tests, (b) for series SS-160-r80, (c) for series SS-240-r160, (d) for series SS-240-a (160); and photos of the test specimen (e) for series SS-160-r80, (f) for series SS-240-r160.

range of 0.01–75.00 mm) on the base plate. The crack width was also measured; however, the detailed evaluation of the crack widths is beyond the scope of this current paper. Typical setups used in the group tests are depicted in Fig. 7.

### 3. Test results and evaluation

In this section, the obtained experimental results are discussed and compared with calculations based on the recommendations given in EN 1992-4 and fib Bulletin 58. The equations for calculating the concrete edge failure load of anchorages in non-cracked concrete  $V_{Rm,c}$  are explained in Section 3.1. The summary of the test results in terms of the

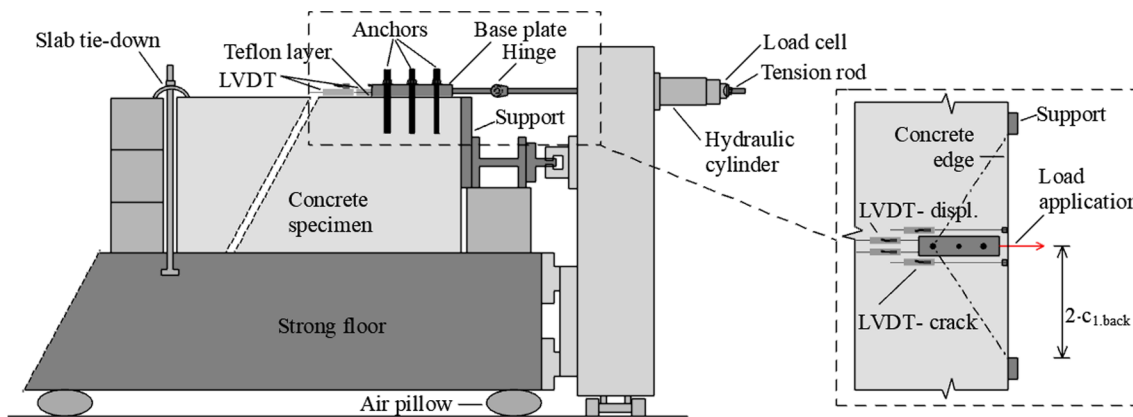


Fig. 6. Schematic drawing of the test setup for anchor groups loaded perpendicular towards the concrete edge.

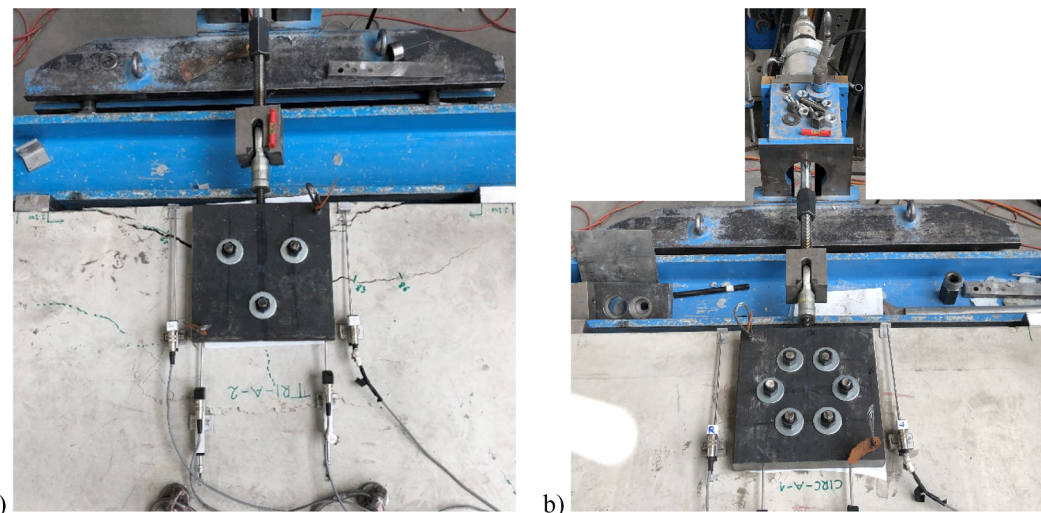


Fig. 7. Typical test setups used for (a) triangular and (b) hexagonal anchor groups loaded perpendicular towards the concrete edge.

Table 3

Summary of the test results on single anchors and anchor groups arranged perpendicular to the edge and loaded perpendicular to the edge.

Test series ID	Mean measured ultimate load <sup>b)</sup>	Mean value of initial stiffness	Calculated mean concrete edge resistance based on EN 1992-4 <sup>c)</sup>		Calculated mean concrete edge resistance based on fib Bulletin 58 <sup>d)</sup>	
			V <sub>u,m</sub>	k <sub>1</sub>	V <sub>Rm,c,EN</sub>	V <sub>u,m</sub> /V <sub>Rm,c,EN</sub>
			[kN]	[kN/mm]	[kN]	[-]
SS-80	25.5	29.8	23.6		1.08	23.6
SS-160	70.1	33.6	57.2		1.23	57.2
SS-240	106.9	26.3	97.7		1.09	97.7
GS-3×1-80-80	107.7	61.6	23.6		4.56	97.7
GS-2×1-80-80	61.9	41.6	23.6		2.62	57.2
GS-2×1-160-80	113.6	44.8	23.6		4.81	97.7
SS-160-r80	71.9	27.9	—		—	—
SS-240-r160	105.0	28.9	—		—	—
SS-240-a(160) <sup>a)</sup>	54.0	16.2	—		—	—

<sup>a)</sup> The test series SS-240-a(SS-160), SS-240-a(SS-160-r80) and SS-240-a(GS-2×1-80-80) are evaluated together as test series SS-240-a(160)

<sup>b)</sup> Crack initiation depends on the actual hole clearance and load distribution.

<sup>c)</sup> Crack initiation assumed from front anchor row.

<sup>d)</sup> Crack initiation assumed from back anchor row.

mean value of the ultimate shear loads V<sub>u,m</sub>, as well as the mean value of the initial shear stiffness k<sub>1,m</sub> for the particular test series is tabulated in Table 3 and Table 4. The initial shear stiffness is defined as the secant stiffness corresponding to 50% of the ultimate load since the load-displacement curve is nearly linear up to this point. Correspondingly, the

initial shear stiffness k<sub>1</sub><sup>i</sup> was calculated for every test as the ratio of 0.5V<sub>u</sub><sup>i</sup> / 8(0.5V<sub>u</sub><sup>i</sup>). The load-displacement curves and the failure modes are given in the following, in the corresponding subsections.

**Table 4**

Summary of the test results of anchor groups of non-rectangular configurations loaded in shear perpendicular to the edge.

Test series ID	Mean measured ultimate load <sup>b)</sup>	Mean meas. ultimate load normalised to $f_{cc} = 25.2 \text{ MPa}$	Mean value of initial stiffness	Calc. mean concrete edge resistance based on EN 1992-4 <sup>c)</sup>	Calc. mean concrete edge resistance based on fib Bul.58 <sup>d)</sup>	
	$V_{u,m}$	$V_{u,m}^*$ <sup>a)</sup>	$k_1$	$V_{Rm,c,EN}$	$V_{Rm,c,fib}$	$V_{u,m}^*/V_{Rm,c,fib}$
	[kN]	[kN]	[kN/mm]	[kN]	[kN]	[ - ]
SS-100	36.7	36.7	25.7	28.2	1.30	28.2
SS-120 <sup>a)</sup>	43.4	41.5	31.1	35.5	1.17	35.5
SS-170	71.0	71.0	37.6	55.8	1.27	55.8
SS-200	83.6	83.6	31.2	69.2	1.21	69.2
SS-240b <sup>a)</sup>	93.8	89.7	34.9	88.1	1.02	88.1
GS-TRI-A	80.1	80.1	77.5	49.2	1.63	88.1
GS-TRI-B	111.3	111.3	69.1	35.5	3.13	105.1
GS-HEX-A	106.2	106.2	74.2(91.6)	36.0	2.95	97.9
GS-HEX-B	92.4	92.4	85.9	21.3	4.34	88.1

<sup>a)</sup> The tests were performed in a different concrete batch compared to the other tests, therefore, to allow a direct comparison of the results, the mean ultimate load was normalised with respect to the concrete compressive strength:  $V_{u,m}^* = V_{u,m} (25.2/27.6)^{0.5}$ .

<sup>b)</sup> Crack initiation depends on actual hole clearance and load distribution.

<sup>c)</sup> Crack initiation assumed from front anchor row.

<sup>d)</sup> Crack initiation assumed from back anchor row.

### 3.1. Calculation of the concrete edge failure load of anchorages in non-cracked concrete

Based on the EN 1992-4 and fib Bulletin 58, the mean shear resistance of an anchorage in case of concrete edge failure can be calculated according to the following equations.

$$V_{Rm,c} = V_{Rm,c}^0 \cdot \frac{A_{c,V}}{A_{c,V}^0} \cdot \Psi_{s,V} \cdot \Psi_{h,V} \cdot \Psi_{ec,V} \cdot \Psi_{x,V} \cdot \Psi_{re,V} \quad (1)$$

Where,

$V_{Rm,c}^0$  is the mean basic resistance in case of concrete edge failure of a single anchor in uncracked concrete is calculated according to Eq. (2)

$$V_{Rm,c}^0 = 1.33 \cdot 2.4 \cdot d_{nom}^\alpha \cdot l_f^\beta \cdot \sqrt{f_{cm}} \cdot c_1^{1.5} \quad (2)$$

$$\alpha = 0.1 \cdot (l_f/c_1)^{0.5} \quad (3)$$

$$\beta = 0.1 \cdot (d_{nom}/c_1)^{0.2} \quad (4)$$

$d_{nom}$  nominal anchor diameter

$l_f$  effective embedment depth;  $l_f = h_{ef}$  in case of a uniform diameter of the shank of the headed fastener and a uniform diameter of the post-installed fastener

$f_{cm}$  mean concrete cylinder compressive strength measured on concrete cylinder of  $\phi = 150 \text{ mm}$  and  $h = 300 \text{ mm}$ , which is convertible from  $f_{cc,150}$  (mean cube compressive strength with side length of  $a = 150 \text{ mm}$ )  $f_{cm} = 0.8 \cdot f_{cc,150}$

$c_1$  edge distance ( $c_1$  = either the edge distance of the front row or edge distance of back row depending on the used approach)

$\frac{A_{c,V}}{A_{c,V}^0}$  ratio, takes into account the geometrical effect of spacing as well as of further edge distances and partly the effect of thickness of the concrete member on the resistance

$A_{c,V}^0$  reference projected area,  $A_{c,V}^0 = 4.5 \cdot c_1^2$

$A_{c,V}$  area of the idealised concrete breakout body, limited by the overlapping concrete cones of adjacent fasteners ( $s \leq 3 \cdot c_1$ ) as well as by edges parallel to the assumed loading direction ( $c_2 \leq 1.5 \cdot c_1$ ) and by member thickness ( $h \leq 1.5 \cdot c_1$ ).

$\Psi_{s,V}$  takes account of the disturbance of the distribution of stresses in the concrete due to further edges of the concrete member on the shear resistance

$\Psi_{h,V}$  takes account of the fact that the concrete edge resistance does not decrease proportionally to the member thickness as assumed by the

ratio  $\frac{A_{c,V}}{A_{c,V}^0}$

$\Psi_{ec,V}$  takes into account a group effect when different shear loads are acting on the individual fasteners of a group (eccentric loading)

$\Psi_{x,V}$  takes account of the influence of a shear load inclined to the edge under consideration on the concrete edge resistance

$\Psi_{re,V}$  takes account of the effect of reinforcement located on the edge

Note that the tests performed within the scope of this current study were carried out in non-cracked concrete without the influences due to further edges, member thickness, eccentricity, inclined loading or reinforcement. Consequently, Eq.(1) simplifies to Eq.(5). When the resistance is calculated based on the EN 1992-4, the failure crack is assumed to initiate from the front row ( $c_1 = c_{1,front}$ ), and if the resistance is calculated based on the fib Bulletin 58, the failure crack is assumed to initiate from the back row ( $c_1 = c_{1,back}$ ).

$$V_{Rm,c} = V_{Rm,c}^0 \cdot \frac{A_{c,V}}{A_{c,V}^0} \quad (5)$$

### 3.2. Results of the experimental investigations

#### 3.2.1. Test results on anchorages of rectangular configurations

The test series according to Table 1 aimed to investigate the relation between the load-displacement behaviour of single anchors with a particular edge distance ( $c_{1,i}$ ) and anchor groups with more anchor rows, having the same corresponding edge distance ( $c_{1,i}$ ,  $i = 1-3$ ). Therefore, for every edge distance of a particular anchor group, reference tests were carried out. The results of the single anchor tests are discussed individually, as well as together with the group tests for comparison. The summary of the test results in terms of the mean value of the ultimate shear loads  $V_{u,m}$  and the mean value of the initial shear stiffness  $k_{1,m}$  is given in Table 3. The corresponding load-displacement curves and the failure crack patterns are discussed in the following subsections.

**3.2.1.1. Reference tests.** Reference tests on single anchors, with 80, 160 and 240 mm edge distance were carried out in test series SS-80, SS-160, SS-240, respectively. As expected, the test results display a strong increase in the failure load with larger edge distance. The initial stiffness  $k_{1,m}$  of the corresponding series SS-80, SS160 and SS-240 were 29.8, 33.6 and 26.3 kN/mm, respectively, which corresponds to a

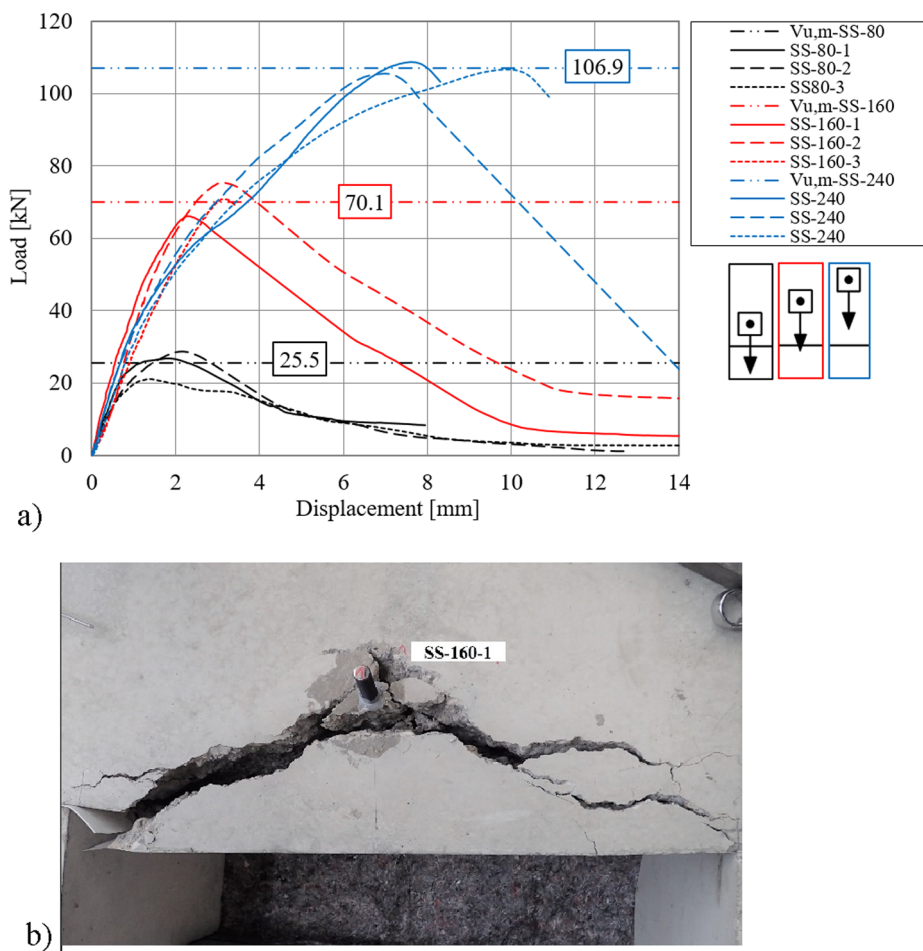


**Fig. 8.** Test series on single anchors (a) load-displacement curves, (b) failure crack pattern of a representative test SS-160-1.

mean value of 29.9 kN/mm. The initial shear stiffness was found to be practically independent of the edge distance, which agrees well with the findings from the literature [20,27]. The load-displacement curves of the reference series are shown in Fig. 8a. The horizontal lines correspond to the mean value of the test results, which are written in the boxes. The failure crack pattern of a representative test is given in Fig. 8b.

### 3.2.1.2. Results of shear tests performed on anchor groups

**3.2.1.2.1. Tests on groups with the equal edge distance for back anchor row ( $c_{1,back} = 240$  mm).** As summarized in Fig. 3 and Table 1, in addition to the reference tests on single anchors, shear tests were also performed on anchor groups of  $3 \times 1$  and  $2 \times 1$  configuration with the edge distance for back anchor row as  $c_{1,back} = 240$  mm. The spacing between the anchors was maintained as 80 mm in both cases, which resulted in the edge distance of front anchor row as  $c_{11} = 80$  mm and  $c_{11} = 160$  mm for  $3 \times 1$  (GS-3  $\times$  1-80-80) and  $2 \times 1$  (GS-2  $\times$  1-160-80) groups, respectively. The load-displacement curves obtained for the series GS-3  $\times$  1-80-80 and GS-2  $\times$  1-160-80 along with the reference single anchor series SS-240 for comparison are shown in Fig. 9. The obtained failure loads for all three series are comparable, which is attributed to equal edge distance for the back anchor row. However, as the number of anchors in a group is increased, the initial stiffness increases.

**Series GS-3  $\times$  1-80-80.** In all three tests of series GS-3  $\times$  1-80-80, the failure crack originated from the back anchor row. However, cracks are also visible originating from the front and middle anchors (Fig. 9b-d). The load redistribution and the crack initiation and propagation

depend on the displacement behaviour of the individual anchors of the group, as well as on the actual hole clearance in the fixture. In all the cases, the hole clearance was measured prior to the test. The load-displacement curves of the tests agree well with the observed crack pattern.

In test 1, the hole clearances for anchor 1, 2 and 3 were measured as 0, 0 and 0.7 mm respectively. In test 1, no crack has formed at the front row, only at the middle and back rows (Fig. 9b). Accordingly, in the beginning, anchor 1 and 2 took up the shear load; and when the applied load reached 50 kN at a displacement of 0.7 mm, the back anchor started to take up the loads as well and an increase in the stiffness in the load-displacement curve can be observed. The crack at the middle anchor developed at an applied load of around 90 kN, after which the stiffness of the group reduced. The failure crack at the back anchor row occurred at an applied load of ca. 99 kN. The peak load of the group was obtained as 99.6 kN.

In test 2, zero hole clearance was measured at the front anchor, 1 mm at the second anchor and ca. 1.5 mm at the third anchor. Fig. 9c shows that in the case of test 2, almost a separate breakout body has formed at the front anchor. This can be explained by relatively large hole clearances at the back rows and by the displacement behaviour of the single anchors of the corresponding anchor rows from the reference series. Due to zero hole clearance, initially, the entire load is resisted by the front anchor only, resulting in a lower stiffness than in case of test 1. The load-displacement curve shows a change in stiffness at an applied load of ca. 50–55 kN load and 1.7 mm displacement. This can be explained by comparing the group behaviour with the behaviour of single anchors tested at different edge distances. The mean failure displacement for the single anchors tested at an edge distance of 80 mm (series

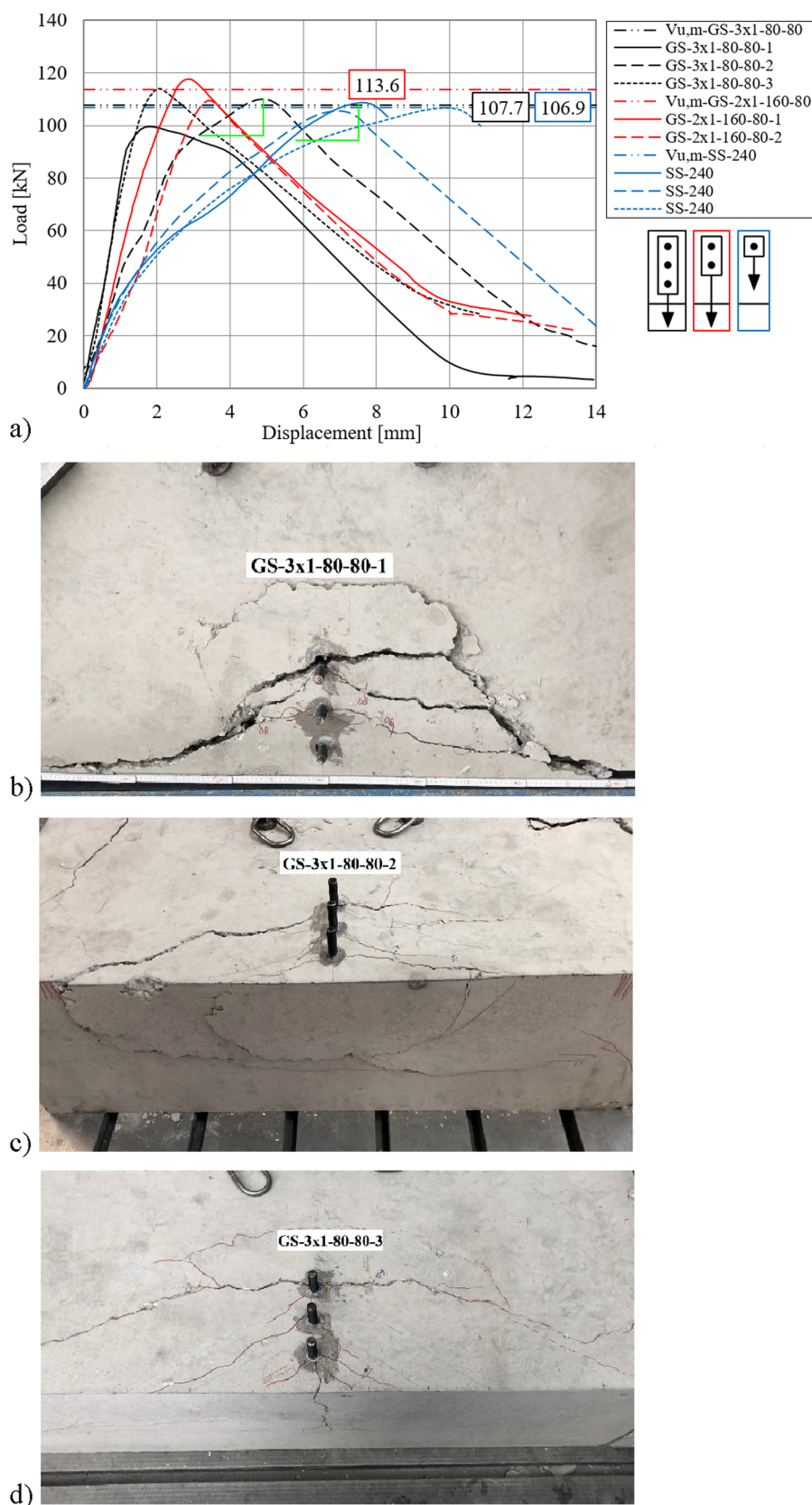


**Fig. 9.** (a) Load-displacement curves of series GS- $3 \times 1$ -80-80 and GS- $2 \times 1$ -160-80 compared with SS-240, (b)-(d) failure crack pattern of series GS- $3 \times 1$ -80-80, (e), (f) failure crack pattern of series GS- $2 \times 1$ -160-80.

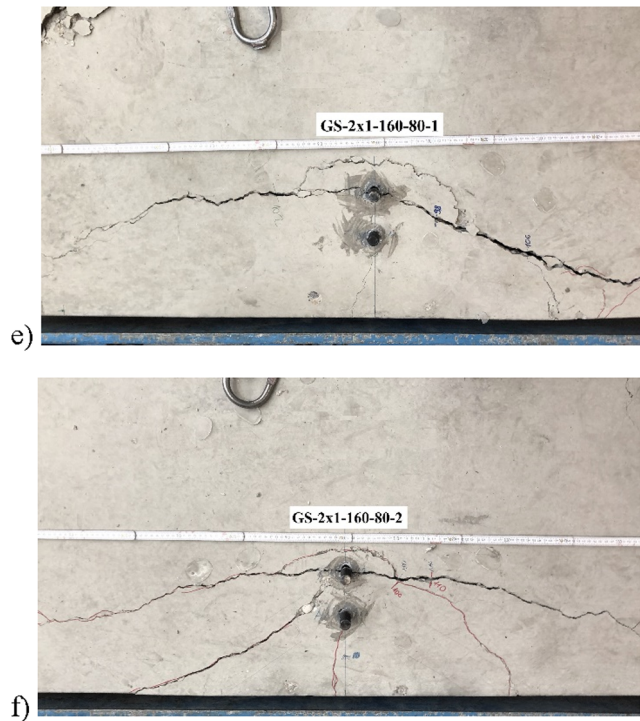


Fig. 9. (continued)

SS-80) was approx. 1.7 mm at  $V_{u,m} = 25.5$  kN (refer Fig. 7a). With a hole clearance of 1 mm at the second anchor, it implies that when the displacement at the front anchor row reaches 1.7 mm, the displacement at the second anchor row would be 0.7 mm, which corresponds to a load of approx. 26 kN taken up by the anchor tested in series SS-160 (edge distance 160 mm). Furthermore, at an applied displacement of 1.7 mm, due to the hole clearance of 1.5 mm, anchor 3 reaches only 0.2 mm displacement (1.7–1.5). This corresponds to approx. 5 kN load in the reference series SS-240. Therefore, at an applied displacement of approx. 1.7 mm, anchor 1 reaches its full capacity ( $\sim 25$  kN), anchor 2 also takes up  $\sim 25$  kN load and the anchor 3 takes up approx. 5 kN or less. The second loss in stiffness is visible on the load-displacement curve at ca. 91 kN applied load and 2.5 mm group displacement. This is attributed to the failure of the second anchor and redistribution of further forces to the back anchor and can again be explained by comparing the behaviour of the group with the behaviour of single anchors. Finally, the back anchor row resisted the load along with the possible residual capacity of anchor 1 and 2. The ultimate load of the group (109.4 kN) was reached at 5 mm displacement. It may be noted that the secant stiffness of the group at failure was almost identical with the secant stiffness of one single anchor with an edge distance of 240 mm, which indicates that the first and second anchors had very low stiffness at the time of reaching the ultimate load of the group.

In test 3, the cracks at all three anchors have formed at the same time, when reaching the peak load. The hole clearance configuration was measured as zero hole clearance at the front row, 0.5 mm at the middle row and ca. 1 mm at the back row. The hole clearance was; however, smaller than the displacement at failure for the corresponding single anchor series SS-160 and SS-240 ( $a_{cl,160mm} = 0.5$  mm  $< \delta(V_{u,c,ss-160}) = 2.5$  mm and  $a_{cl,240mm} = 1.0$  mm  $< \delta(V_{u,c,ss-240}) = 8$  mm). Therefore, the load distribution was ideal; and from 1 mm displacement onwards, all the three anchors were loaded together, contributing assumedly with the same amount of force, which is also indicated by the progression of the load-displacement curve.

The failure load calculated according to the approach given in fib Bulletin 58 assuming the failure crack from the back row is in a good agreement with the test results. The calculated mean failure load is

approx. 10% lower than the experimentally obtained mean failure load. On contrary, the calculation based on the approach given in EN 1992-4 assuming the failure crack from the front anchor row is over-conservative (see Table 3) due to neglecting the force redistribution to the further anchor rows.

An evaluation of the results of the tests performed on  $3 \times 1$  anchor groups highlight the importance of considering the displacement behaviour of individual anchors within an anchor group while evaluating the performance of anchor groups. In this way, not only the peak load but also the redistribution of forces, change in stiffness due to the development of cracks and the complete load-displacement response of the anchor groups can be estimated. Accordingly, different failure criteria for different limit states (such as serviceability and ultimate) can be set and a rational design approach can be developed. At present, no consideration of the displacement behaviour of the anchors is given in the existing codes and standards.

**Series GS-2 × 1-160-80.** Two tests were carried out on the test series GS-2 × 1-160-80 with 160 mm edge distance of the front row and 80 mm anchor spacing, resulting in the edge distance of back anchor row as 240 mm. As expected, the peak load was similar but the stiffness was lower in the group tests than that obtained with the groups of  $3 \times 1$  configurations (Fig. 9a).

In test 1, zero hole clearance was measured at both front and back anchors. This anchor group can be considered as an anchor group without hole clearance. The curve progression and crack pattern indicate that the shear force was distributed between both anchors almost equally up to the failure load. This agrees with the findings in the literature for groups without hole clearance. According to [7,21,28–30], when an anchor group with a  $s_1 / c_{1,1} < 1.0$  ratio is loaded in shear perpendicular to the concrete edge, the crack origination from the front row is suppressed by the compression field, which is originating from the back anchor row.

In test 2, ca. 1 mm hole clearance was measured at the front anchor and zero hole clearance at the second anchor. Since the hole clearance at the front anchor was smaller than the displacement at failure for the corresponding single anchor series SS-160 ( $a_{cl,160mm} = 1.0$  mm  $< \delta(V_{u,c,ss-160}) = 2.5$  mm), the load distribution was ideal. The back anchor was loaded first and from ca. 1 mm displacement onwards, both anchors were loaded together. This is also reflected in the curve progression, which shows an increase in the group stiffness (Fig. 9a). There are no cracks visible originating from the front anchor, and the failure crack originates from the back anchor (Fig. 9f).

### 3.2.1.2.2. Tests on groups with the equal edge distance for back anchor row ( $c_{1,back} = 160$ mm) Series GS-2 × 1-80-80

Three tests were carried out with the anchor group configuration of  $2 \times 1$ , having 80 mm edge distance in the front row and 80 mm anchor spacing, resulting in an edge distance of the back anchor row as 160 mm. This corresponds to a ratio,  $s_1/c_{1,1} = 1.0$ . The load-displacement curves of the series GS-2 × 1-80-80 along with the reference single anchor series SS-160 are plotted in Fig. 10a. Fig. 10b-d show that in all the tests, the failure crack originated from the back anchor row. In tests 1 and 2, no major change in the stiffness of the curves is noticed until peak load, while for test 3, after reaching a load of 27.4 kN, a drop in the load with increasing displacement followed by a re-rise of the load-displacement curve is observed. This can again be explained through the consideration of anchor displacements and hole clearances.

In test 1, anchor 1 had a zero hole clearance and was activated first, while anchor 2 had a nominal clearance of 0.5 mm and therefore, from 0.5 mm displacement, both the anchors took up the shear forces. The front anchor developed a crack at a load close to 25 kN (approx. failure load of the single anchor tested with an edge distance of 80 mm) and its stiffness decreased. From this point onwards, the back anchor started to take up higher forces compared to the front anchor to fulfil the equilibrium (equal displacement & different stiffness, different forces). The ultimate load corresponds to the failure crack appearing from the back anchor.

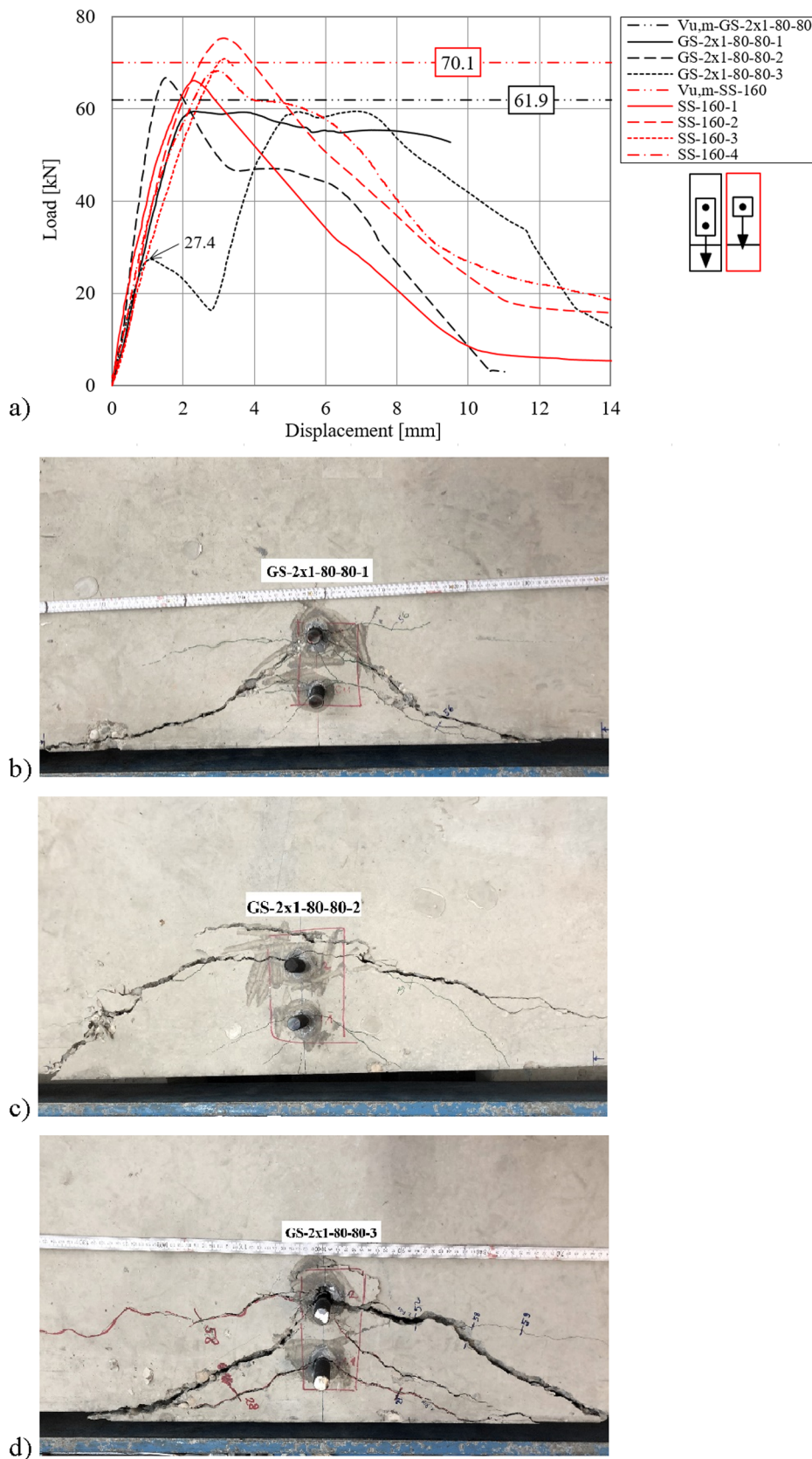


**Fig. 10.** a) Load-displacement curves of series GS- $2 \times 1$ -80-80 compared with SS-160, (b)-(d) failure crack pattern of series GS- $2 \times 1$ -80-80.

In test 2, both the anchors were activated at the same time due to almost zero hole clearance and consequently, the shear load was initially distributed to both anchors equally up to ca. 80% the ultimate

load of the front anchor (compare Fig. 8a). It is attributed to the reduction in stiffness of the front anchor upon reaching ca. 80% of its ultimate load. From this point onwards, the back anchor could take up

slightly higher loads until the failure of the front row to satisfy the equilibrium. The failure of the anchorage corresponds to the appearance of failure crack from the back anchor row.

Test 3 is a good example for anchorages having unfavourable hole configuration, where due to hole clearance the entire shear load is distributed initially only to the front anchor. In this test, anchor 1 had zero hole clearance but anchor 2 had a relatively large hole clearance of 2 mm. Consequently, initially, only the front anchor takes up the shear load. The first peak in Fig. 10a corresponds to the failure of the front anchor (27.4 kN and 1 mm) and to the first cracking at the front anchor (Fig. 10c). When the applied shear displacement reached ca. 2 mm, anchor 2 was activated. The group force corresponds from this point to the shear force taken up by second anchor and the residual capacity of the front anchor. From 2.8 mm group displacement, the shear resistance of the group rises again. The peak load corresponds to the failure crack appearing from the back anchor.

The mean ultimate load, calculated based on the fib Bulletin 58 assuming the failure crack from the back anchor is only 8% lower than the mean experimental value, while the mean failure load calculated based on the EN 1992-4 assuming the failure crack from the front anchor is over-conservative (see Table 3). However, in the case of test 3, the calculated failure load according to EN 1992-4 matches reasonably well with the first peak of 27.4 kN. These tests highlight the need for a displacement-based evaluation method. It can be seen that even after the first cracking, the anchors are able to transfer forces. The first cracking and first peak might limit the design for SLS; however, when the entire load-displacement behaviour of anchor groups is evaluated, a displacement criterion can be worked out. Consequently, only anchor groups with a particular displacement behaviour and hole clearance pattern would be subjected to the limitations.

### 3.2.2. Test series on single anchors with recess

The tests series SS-160-r80 and SS-240-r160 correspond to the experiments carried out on single anchors at an edge distance of 160 mm and 240 mm, respectively with the corresponding recess of 80 mm and 160 mm in the front (refer to Table 1 and Fig. 3). It is clear from the test results that the presence of a recess in front of the anchor has no significant influence on either the ultimate resistance or the stiffness of the anchors (Fig. 11a). This can be attributed to the fact that the concrete recess does not affect the breakout surface and the stress distribution in the load transfer area of the anchor is not disturbed. The failure pattern of one representative test is depicted in Fig. 11b. The failure crack propagates to the support, parallel to the recess and the depth of the breakout body is ca.  $1.5c_1$ .

In test series SS-240-r160, the tested anchor was installed at an edge distance of 240 mm. The recess in the front of the anchor was cast with the dimensions of the theoretical breakout body of an anchor with 160 mm edge distance. Again, no significant influence of the recess is observed on the load-displacement behaviour of the anchors (Fig. 12a). This confirms again that when the ultimate load is reached, the stress distribution in the load transfer zone of the anchor is not disturbed; only the compression field is different due to the recess. The failure pattern of one representative test is depicted in Fig. 12b. In principle, the failure crack runs parallel to the surface of the recess.

### 3.2.3. Test series in pre-damaged concrete specimen

The test series SS-240-a-160 were carried out on single anchors with an edge distance of 240 mm. However, before the installation, tests with an edge distance of 160 mm have been already carried out on  $2 \times 1$  anchor groups (series GS- $2 \times 1$ -80-80), single anchors (series SS-160) and single anchors with a recess in the front (series SS-r80). Before the new tests, the breakout body was removed and the anchors were installed only in the location, where no damage was visible at the concrete surface. A typical example is given in Fig. 13 showing the pre-damaged condition with a new anchor installed at 240 mm edge distance behind the failure surface of a  $2 \times 1$  anchor group (GS- $2 \times 1$ -80-

80-2).

The load-displacement curves along with the concrete breakout bodies are shown in Fig. 14. For comparison, the reference single anchor tests with the corresponding edge distance (240 mm) are also plotted in the graph. The ultimate load reached in this series scatters between 40.7 and 78.1 kN. The lowest value corresponds to 38%; the highest value corresponds to 73% of the mean ultimate load obtained in the reference series. Such a large scatter in the test results is attributed to the fact that the “residual” resistance of the anchor depends on the pre-damage in the concrete. Even though not visible on the surface, due to the lateral tensile stresses generated due to applied loading on the anchor previously installed and tested, the concrete behind the anchor gets certain damage. The amount of damage varies from case to case and is not quantifiable. No significant difference was observed whether the new anchor was installed after a group test ( $2 \times 1$ ), or after a single anchor test, or after a single anchor test with recess, provided the edge distance to the back anchor or the single anchor remains same. It can be assumed that the cases with larger damage to the concrete resulted in lower values of resistance for this series and vice-versa.

Even though the minimum distance between the anchor and the recess created due to pre-damage was 80 mm, in all cases, the failure load was higher than the failure load corresponding to the failure of the anchor with 80 mm edge distance. This is attributable to the larger concrete breakout surface in this case. The mean initial stiffness is 16.2 kN/mm, which is 62% of the stiffness of the reference series. The 38% loss of stiffness can be attributed to the cracked concrete condition.

These results highlight a major difference between the behaviour of anchors with a recess created due to damage of the previously loaded anchor and with a recess created at the time of casting. This can be explained by the fact that in case of the tests with recess, due to the creation of the recess during casting itself, there was no disturbance to the stress field around the tested anchor. Since the surface of the breakout body remains essentially the same as in case of tests without recess, the capacity of the anchor is also practically unchanged. However, in case of the tests with pre-damage, the tensile stresses generated perpendicular to the direction of the applied shear load on the anchor tested first, leads to a stress disturbance around the later installed anchor. This disturbance of stresses leads to a reduction in the failure load and stiffness of the anchor installed and tested in pre-damaged concrete, similar to as expected for the anchors tested in cracked concrete.

### 3.2.4. Test results on anchor groups of non-rectangular configurations

The test series according to Table 2 were performed to investigate the behaviour of anchor groups of non-rectangular configurations. Furthermore, similar to the series with rectangular configuration, for every edge distance of a particular anchor group, reference tests were carried out. The summary of the test results in terms of the mean value of the ultimate shear loads  $V_{u,m}$  and the mean value of the initial shear stiffness  $k_{1,m}$  is given in Table 4. The corresponding load-displacement curves and the failure crack patterns are given in the following subsections.

**3.2.4.1. Reference tests.** Reference tests were carried out on single anchors according to Table 2 with edge distances of 100, 120, 170, 200 and 240 mm (test series SS-100, SS-120, SS-170, SS-200, SS-240b). The edge distances for reference tests were selected on the basis of the edge distances of various anchor rows in case of groups tested. The load-displacement curves obtained from the reference tests are plotted in Fig. 15a. As expected, the ultimate loads increase with increasing edge distance. The initial stiffness  $k_{1,m}$  of the corresponding series SS-100, SS-120, SS-200 and SS-240 are 25.7, 31.1, 37.6, 31.2 and 34.9 kN/mm, respectively, which corresponds to a mean value of 32.1 kN/mm. The value of 32.1 is comparable with 29.9 kN/mm measured in the test series according to Table 3. Therefore, the initial shear stiffness can be

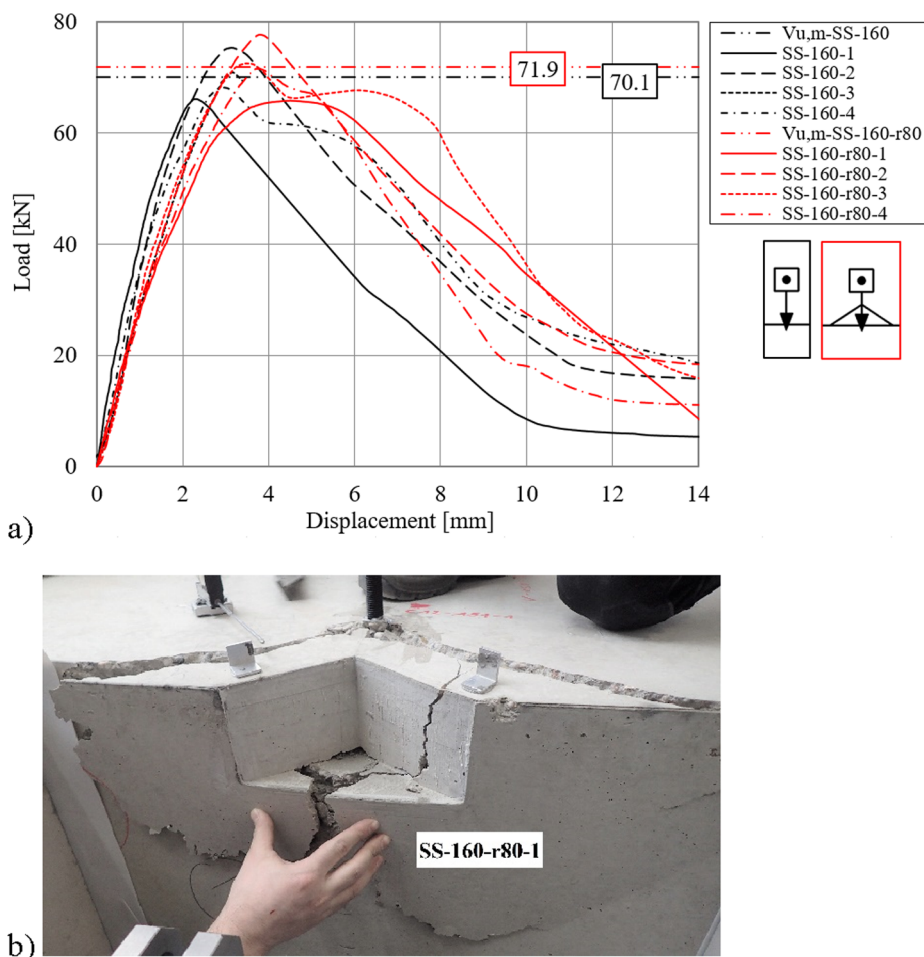


**Fig. 11.** Comparison of reference tests on single anchors with tests with recess (a) load-displacement curves, and (b) failure crack pattern of SS-160-r80-1.

considered as relatively independent of the edge distance. The failure crack pattern of one representative test is shown in Fig. 15b. The failure cracks correspond to the typical concrete edge breakout. The experimentally obtained mean ultimate loads were in reasonable agreement with the calculated mean failure loads according to the CGD Method.

**3.2.4.2. Anchor groups with triangular anchor configuration.** In series GS-TRI-A and GS-TRI-B, shear loading tests were carried out close to the concrete edge using the same base plate and having the same edge distance of the anchor rows. However, in series GS-TRI-A, two anchors were located in the front row and one anchor in the back row, whereas in series GS - TRI - B, one anchor was installed in the front row and two anchors in the back row (Refer to Fig. 4a). Note that this configuration is not covered explicitly by the current design standards. Nevertheless, if the current approaches are extended to triangular groups, the approach given in EN 1992-4, would result in higher concrete edge resistance for the configuration with two anchors in the front row, while according to the design approach given in fib Bulletin 58, the failure load for the configuration with two anchors in the back row would result in higher concrete edge resistance. As can be seen from Table 4, the approach given in fib Bulletin 58 leads to a reasonably good agreement with the test results, while the approach given in EN1992-4 leads to over-conservative values of the calculated failure loads.

The corresponding load-displacement curves of the series and the failure crack patterns are given in Fig. 16. The initial part of the load-displacement curves clearly shows that the initial stiffness of the group is relatively independent of the anchor configuration. This is due to the

fact that the total number of anchors is the same for both series, and the shear stiffness is almost independent of the edge distance.

**GS-TRI-A.** Test series GS-TRI-A (Fig. 4a) was performed on anchor groups of triangular configuration with two anchors in the front row ( $c_{1,1} = 120$  mm) and one anchor in the back row ( $c_{1,2} = 240$  mm) having arbitrary hole clearance configuration. The mean failure load obtained from the experiments was 80.1 kN. The load-displacement curves, as well as the photos of the crack pattern, indicate that the displacement behaviour of the individual anchors and the hole clearance pattern have a significant influence on the group behaviour.

In test 1, the hole clearance pattern corresponded to  $a_{cl} = 1$  mm for anchor 1, and  $a_{cl} = 0$  mm for anchors 2 and 3. This is in agreement with the curve progression and crack pattern. It was observed during the test that initially, the crack originates from anchor 2 and anchor 3, whereas the crack at anchor 1 develops only together with the crack from the back anchor. At ca. 70 kN load and 1.1 mm displacement, a change in the stiffness can be observed in the load-displacement curve.

In test 2, the anchors in the front row were loaded first and equally, and the anchor in the back row had ca. 1 mm gap and was activated later. The influence of hole clearance can be indicated both in the curve progression and in crack pattern as shown in Fig. 16c. The crack at the front row has developed when reaching 60–65 kN and 1 mm displacement. A change in stiffness is also visible on the load-displacement curve. This can be attributed to the fact that when anchor 3 started taking up higher forces, the anchors in the front row had much smaller stiffness and were already in the post-peak phase, furthermore, the stiffness of the back anchor was also strongly influenced by the cracks at the front anchors. The failure crack from the back anchor partly went parallel to and partly joined the cracks previously appearing from the

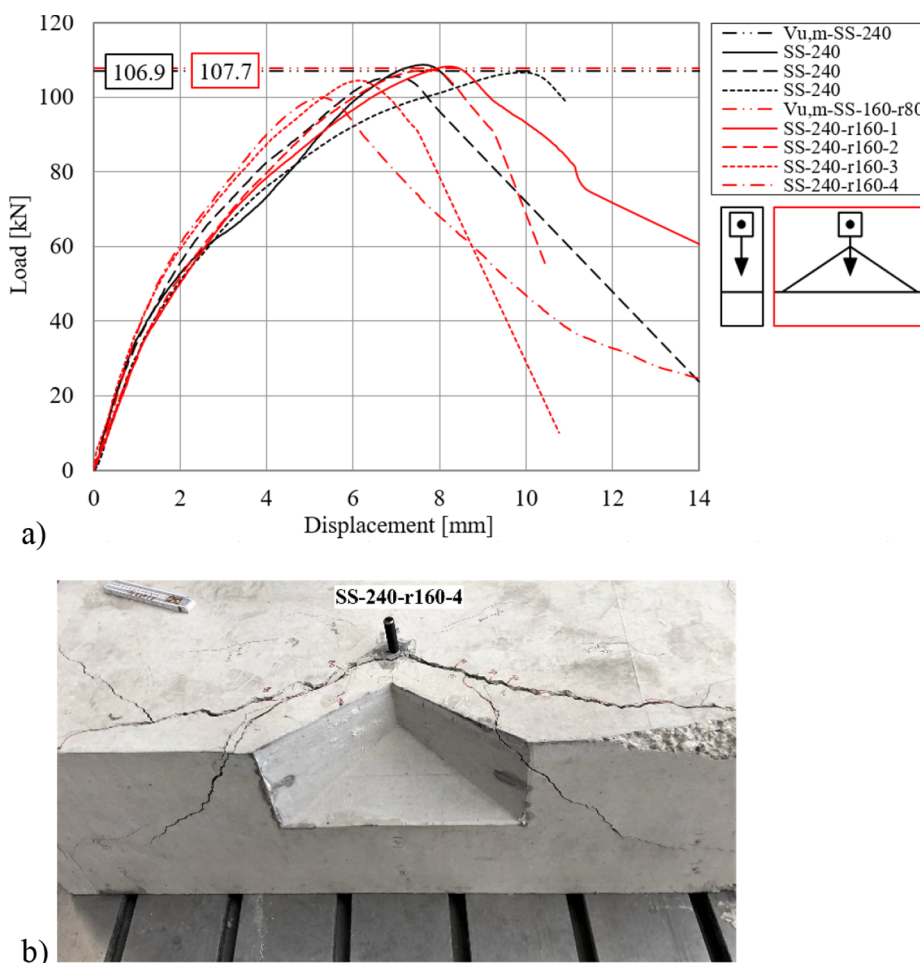


Fig. 12. Comparison of reference tests on single anchors with tests with recess: (a) load-displacement curves, (b) failure crack pattern of SS-240-r160-4.



Fig. 13. Pre-damaged concrete after installation: test SS-240-a(GS-2x1-80-80)-2.

front row. The cracks at the side opposite to loading direction have developed only after the failure of the group due to the uplift of the base plate. The failure load, as well as displacement at the peak load, are in good agreement with the corresponding values obtained in the reference tests on single anchor series SS-240b.

The anchors in test 3 were installed with the most unfavourable hole clearance pattern. The anchors in the first row had zero hole clearance and were activated immediately on application of the load but anchor 3 was activated only after a displacement of 1.5 mm, due to the hole clearance ( $a_{cl,3} = 1.5$  mm). This is clearly visible in Fig. 16a and d. The first peak of the group was reached when the anchors in the front row failed at 62.5 kN and 0.9 mm. From this point onwards, the crack at the front row started widening from  $\Delta w = 0.4$  mm and reached a value of

$\Delta w = 1.4$  mm until the third anchor was activated. When anchor 3 started taking up the shear force, the group resistance again increased and the widening of the cracks slowed down. The ultimate load for the group was obtained as 70.4 kN, which is considerably less than measured in the reference series (SS240b) and can be attributed to the presence of wide cracks at the front row. The width of the cracks from the front anchor row measured at the failure load was equal to the group displacement. The pronounced cracking at front anchor had a big influence on the load distribution to the back row.

**GS-TRI-B.** Test series GS-TRI-B was performed on anchor groups of triangular configuration with one anchor in the front row ( $c_{1,1} = 120$  mm) and two anchors in the back row ( $c_{1,2} = 240$  mm) having arbitrary hole clearance configuration (see Fig. 4a). The mean failure load obtained from the experiments was 111.3 kN. The curve progression is very similar in all three cases. This can be due to the fact that only one anchor is installed in the front row and the possible cracking in the front row has a smaller influence on the group performance.

In the case of test 1, the hole clearance configuration corresponded to 0 mm, 0.5 mm and 0.5 mm for the anchors 1, 2 and 3, respectively. In the beginning, only anchor 1 took up the shear load and then from 0.5 mm displacement, the anchors in the back row started also resisting the forces. The first cracking occurred when the group reached a load of 80 kN. The failure crack initiated from the back anchor row as depicted in Fig. 16e.

Test 2 is an example for the favourable hole clearance pattern because the hole clearance of the anchors in the back row was 0 mm, whereas anchor 1 in the front row had ca. 1 mm hole clearance. Consequently, the back anchors were loaded first and equally. The

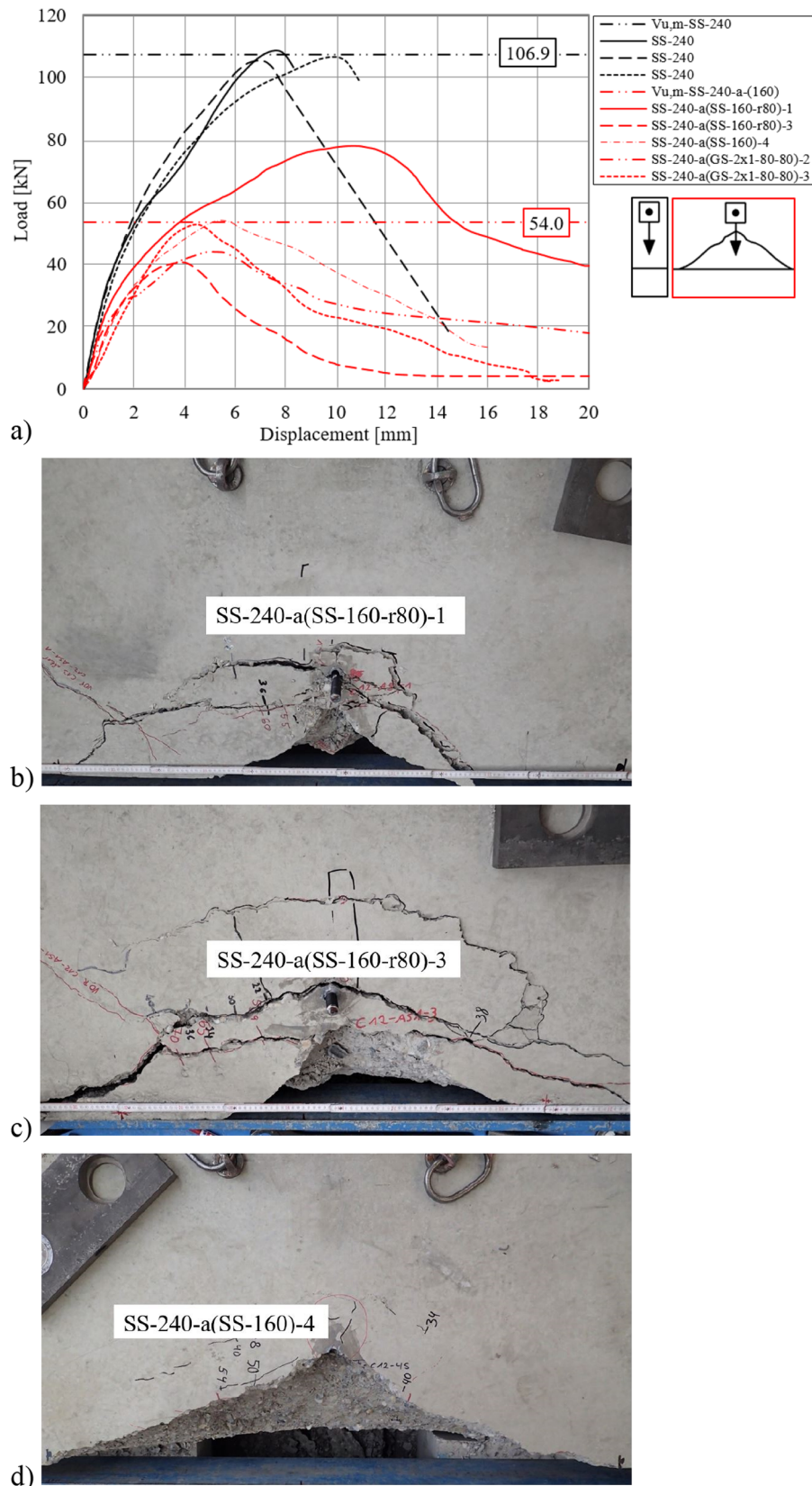


**Fig. 14.** Comparison of reference tests on single anchors with tests in pre-damaged concrete: (a) load-displacement curves, (b)–(f): failure crack pattern of series SS-240-a(160).

curve progression shows an increase in the group stiffness from 1 mm displacement, which suggests the activation of the front anchor (Fig. 16a). There are no cracks visible originating from the front anchor,

and the failure crack originates from the back row (Fig. 16f).

In test 3, the front anchor was activated first and then at 0.5 mm displacement (= hole clearance of back row) the back row started

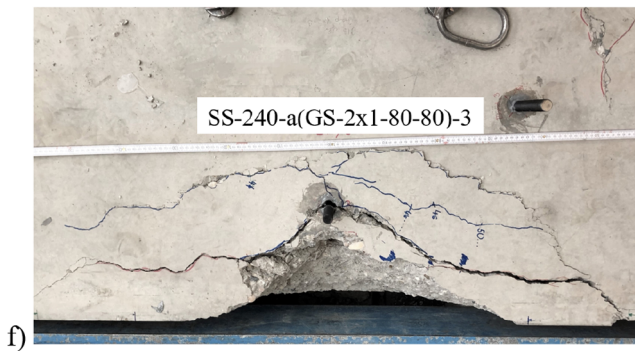


Fig. 14. (continued)

taking up forces. This is also indicated by the increase in stiffness in the load-displacement curve (Fig. 16a). The ultimate load of the group is almost 3-times the failure load of a reference single anchor test with 120 mm edge distance. Although a hairline crack is visible at the front anchor, the failure crack originated from the back anchor row.

**3.2.4.3. Anchor groups with hexagonal anchor configuration.** In series GS-HEX-A and GS-HEX-B, shear loading tests were carried out close to the concrete edge on anchor groups of hexagonal configuration with random hole clearance pattern (depending on the installation accuracy). The six anchors were installed in three rows in test series GS-HEX-A, with two anchors per row, forming a hexagon (Refer Table 2). The edge distances of the corresponding anchor rows were 101, 171 and 240 mm. In the case of series GS-HEX-B, the base plate was rotated by 90° and the anchors were installed in four anchor rows, having one anchor in the front and back row, and two anchors each in the middle rows. The corresponding edge distances were 80, 120, 200 and 240 mm for 1st, 2nd, 3rd and 4th anchor row, respectively. For the easier presentation of the results, the hole clearance pattern is given in Table 5 and in Fig. 17b-g.

It is shown in Table 4 that the approach given in fib Bulletin 58 (failure crack from back anchor row) leads to a reasonably good agreement with the test results, whereas the approach given in EN1992-4 (failure crack from front anchor row) leads to over-conservative values of the calculated failure loads. The corresponding load-displacement curves of the series and the failure crack patterns are given in Fig. 17.

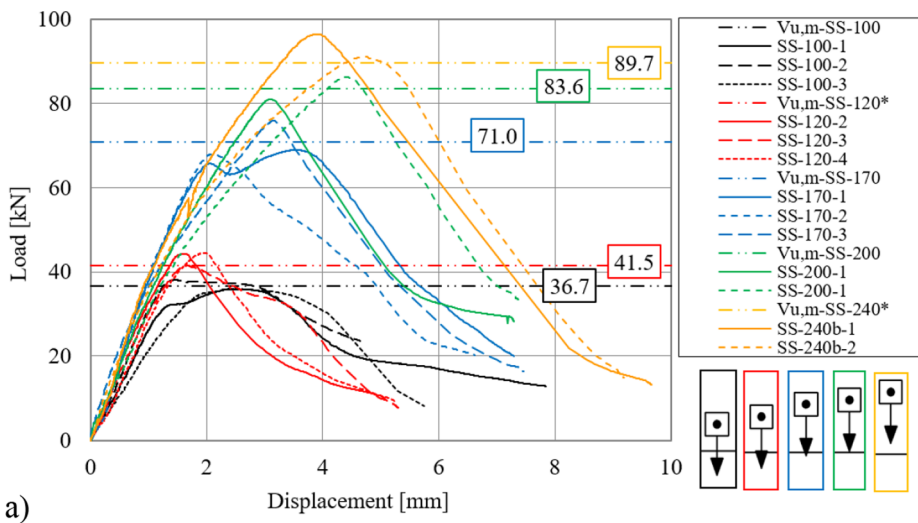
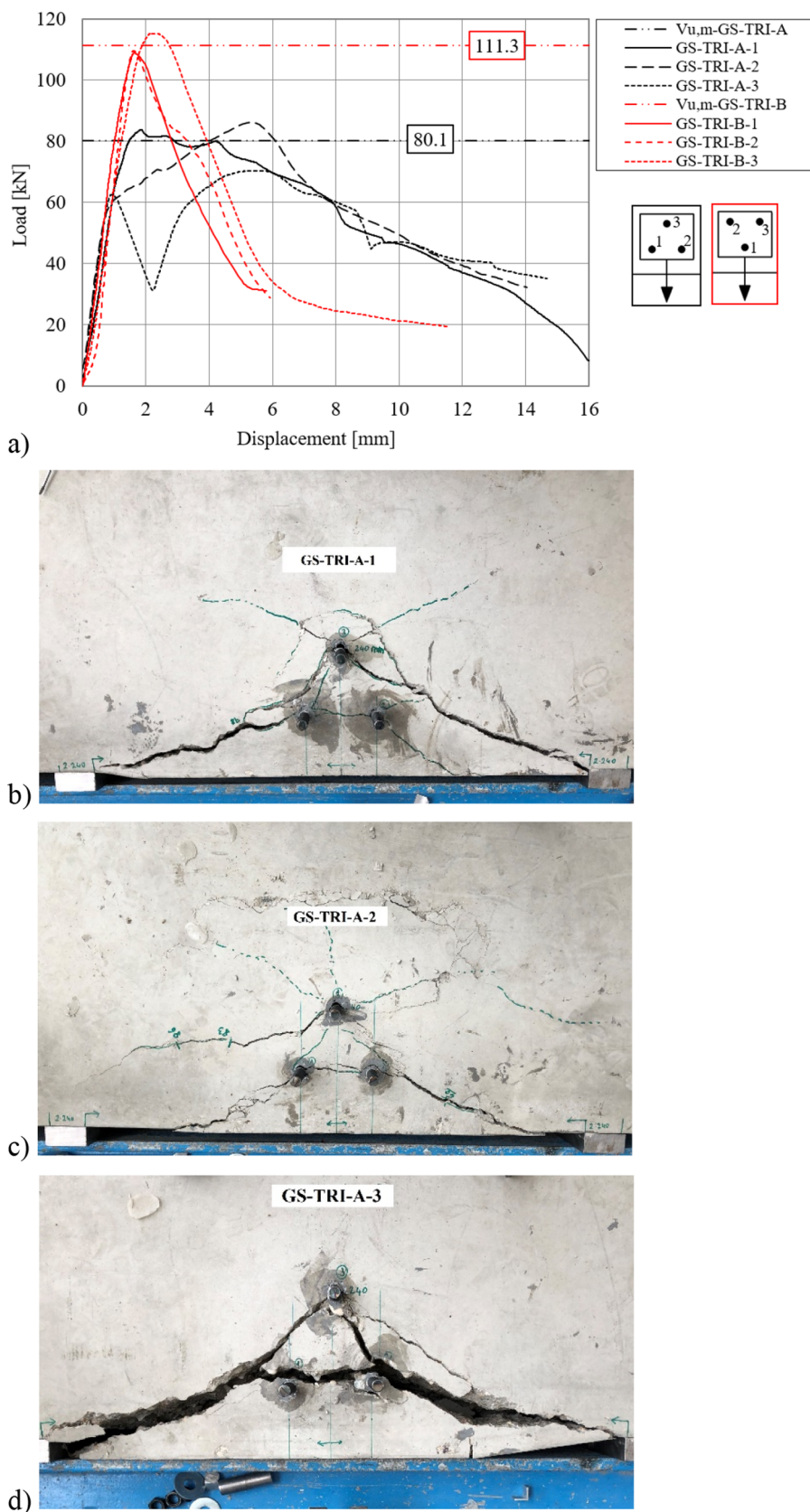


Fig. 15. Test series on single anchors (a) load-displacement curves, (b) failure crack pattern of a representative test SS-170-1.



**Fig. 16.** Test series with triangular configuration (a) load-displacement curves, and failure crack pattern of test (b) GS-TRI-A-1, (c) GS-TRI-A-2, (d) GS-TRI-A-3, (e) GS-TRI-B-1, (f) GS-TRI-B-2, (g) GS-TRI-B-3.

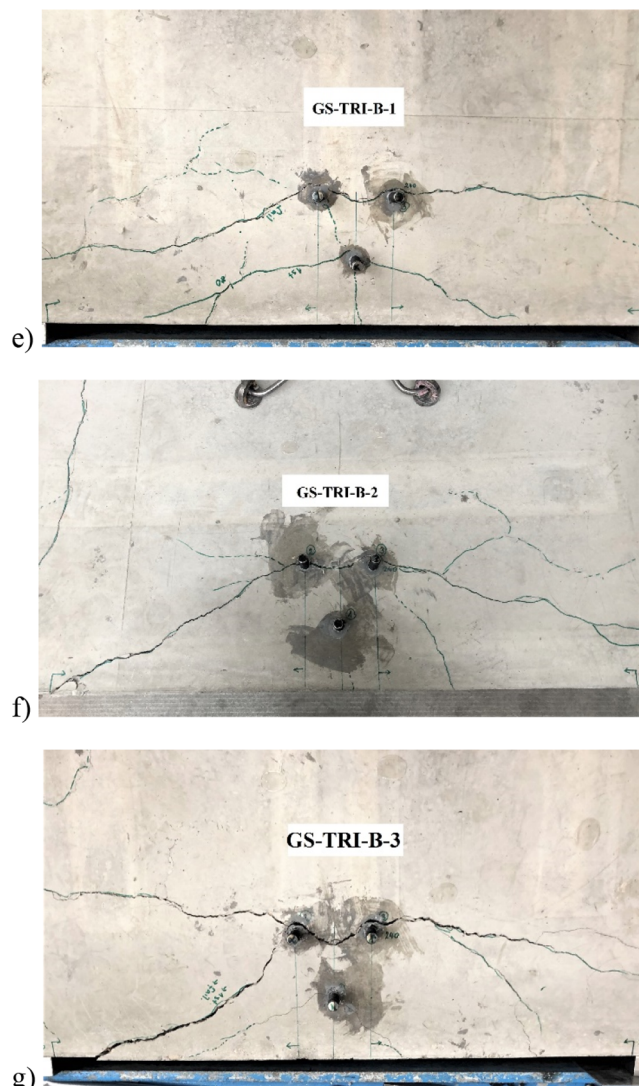


Fig. 16. (continued)

**Table 5**  
Hole clearance pattern for series GS-HEX-A and GS-HEX-B.

Test ID	$a_{cl,1}$	$a_{cl,2}$	$a_{cl,3}$	$a_{cl,4}$	$a_{cl,5}$	$a_{cl,6}$
	[mm]	[mm]	[mm]	[mm]	[mm]	[mm]
GS-HEX-A-1	0	0	1.0	0.5	1.5	1.5
GS-HEX-A-2	0	1.0	1.0	0.5	2.0	1.0
GS-HEX-A-3	1.5	0	1.0	1.5	1.5	1.5
GS-HEX-B-1	0	2	0	1.0	1.5	1.5
GS-HEX-B-2	0	1.0	0.5	1.5	1.5	0.5
GS-HEX-B-3	1.5	0.5	0	2	2	0

It was observed that with the same number of anchors but different anchor pattern, the mean ultimate load was 15% higher in case of test series GS-HEX-A compared to series GS-HEX-B. This is due to the fact that in both series, the edge distance of the back row was 240 mm, however, in series GS-HEX-A, two anchors were placed in the back row with a spacing of 80 mm, which increases the activated concrete body.

**GS-HEX-A.** Test series GS-HEX-A (Fig. 4b) was performed on anchor groups of hexagonal configuration with two anchors in each anchor row with arbitrary hole clearance configuration (Table 5).

In the case of test 1, the first anchor row was activated first. The force redistribution to the further anchors could take place since the hole clearance of the second row (0.5 mm) was considerably smaller

than the displacement at failure of the front row (ca. 1.3 mm considering a higher stiffness for two anchors - derived from the reference single anchor tests SS-100). The third activated anchor was anchor 4 of the second row at 0.5 mm displacement, whereas anchor 3 in the second row was active from 1 mm group displacement. The first crack was observed at the front row at an applied load of 45 kN. The crack has opened up to ca. 0.1 mm width and the third anchor row activated after further 0.5 mm displacement due to the hole clearance pattern. These can also be indicated in the curve progression in Fig. 17a, where after a plateau at approx. 45 kN the load-displacement curve rises again. Finally, the failure crack originated from the back anchor row and the group failed at a shear load of 110.4 kN. The symmetric crack pattern agrees well with the measured hole clearance pattern (Fig. 17b).

The measured hole clearance pattern in case of test 2 was not symmetric, which is also reflected in the developed crack pattern (Fig. 17c). First, anchors 1 and 4, then anchors 2, 3 and 6, and finally, anchor 5 was activated. Correspondingly, the first cracks developed from anchors 1 and 4. The cracks widened originating from anchors 1, 4 and 6 at an applied shear load of ca. 90 kN, and the failure crack has developed from anchor 6 from the back row at 100.2 kN. The curve progression in Fig. 17a shows that the force distribution was optimal and the redistribution was possible once an anchor was overloaded due to attainment of high forces. This is due to the fact that the hole clearance was in all cases smaller than the failure displacement of the corresponding individual anchor.

The behaviour of test 3 is very similar to test 2 up to ca. 95 kN, due to the same number of anchors, which contribute to the load transfer. According to the hole clearance pattern, first, anchor 2, next, anchor 3, and then all other four anchors transferred the load. The first cracks occurred at ca. 100 kN (Fig. 17d), which can also be indicated in the curve progression, with the reduction of stiffness of the group. This can be attributed to the failure of the first loaded anchors 2 and 3. The ultimate load of the group was reached when the capacity of the back anchors was utilised and the failure crack propagated from the back anchor row. This means that even if cracks at the front and middle rows have developed, the shear forces could be redistributed to the back anchor rows.

**GS-HEX-B.** Test series GS-HEX-B (Fig. 4b) was performed on anchor groups of hexagonal configuration with one anchor in the first and fourth rows and two anchors in the second and third anchor rows having random hole clearance pattern (Table 5).

In test 1, the hole clearance was measured to be zero for anchors 1 and 3. This means that at the onset of loading these two anchors were active and the first cracks also appeared to initiate from them at an applied load of 50 kN. Due to the cracking and increasing group displacement, further anchors started to contribute. The third crack originated from anchor 4, which had 1 mm hole clearance. With further loading, cracking was observed originating from anchor 5, when the group reached 80 kN. Finally, the shear force was redistributed to anchor 6, and a group capacity of 91.2 kN was reached. This value corresponds well to the calculations assuming the failure crack originating from the back row. The load-displacement curve obtained in test 1 (Fig. 17a) reflects the behaviour of the anchor group. Furthermore, the crack pattern is in a good agreement with the hole clearance pattern (Fig. 17e).

In the case of test 2, anchor 1 was activated first but already after 0.5 mm displacement, anchors 3 and 6, and later anchor 2 started resisting the forces. This can be indicated in the curve progression and stiffness. The first loss of stiffness is visible when the group reached 1 mm displacement (70 kN), which corresponds also to the first cracking initiating from anchor 2. No cracks are visible originating from the third anchor row, which can be explained by the hole clearance pattern of this row ( $a_{cl} = 1.5$  mm) (see Fig. 17f). The ultimate load of the group was measured 90.1 kN, which corresponds to the calculated value assuming a failure crack from the back anchor row.

The anchors were installed in a favourable hole clearance pattern in

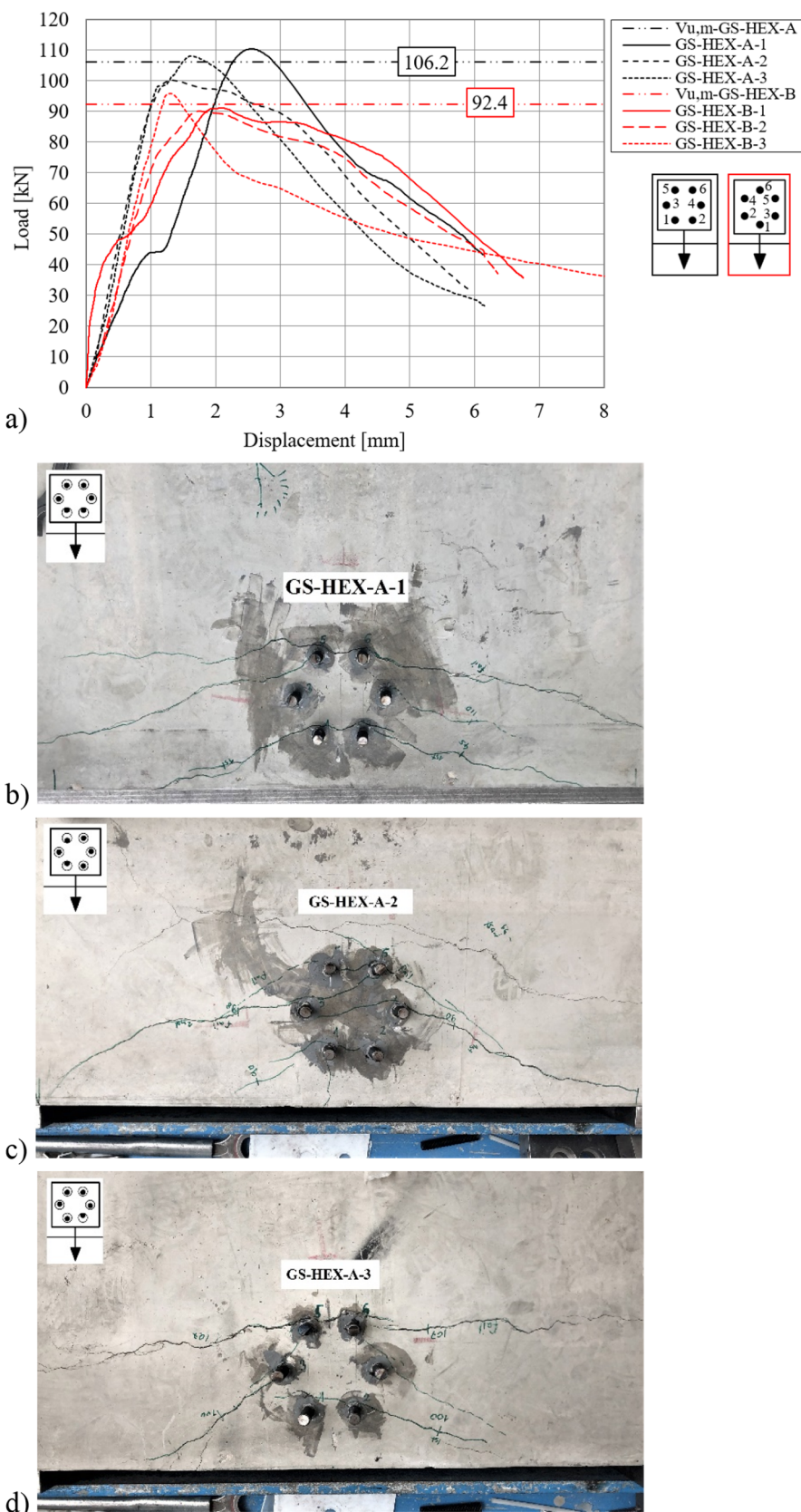


**Fig. 17.** Test series with triangular configuration (a) load-displacement curves, and failure crack pattern of test (b) GS-HEX-A-1, (c) GS-HEX-A-2, (d) GS-HEX-A-3, (e) GS-HEX-B-1, (f) GS-HEX-B-2, (g) GS-HEX-B-3.

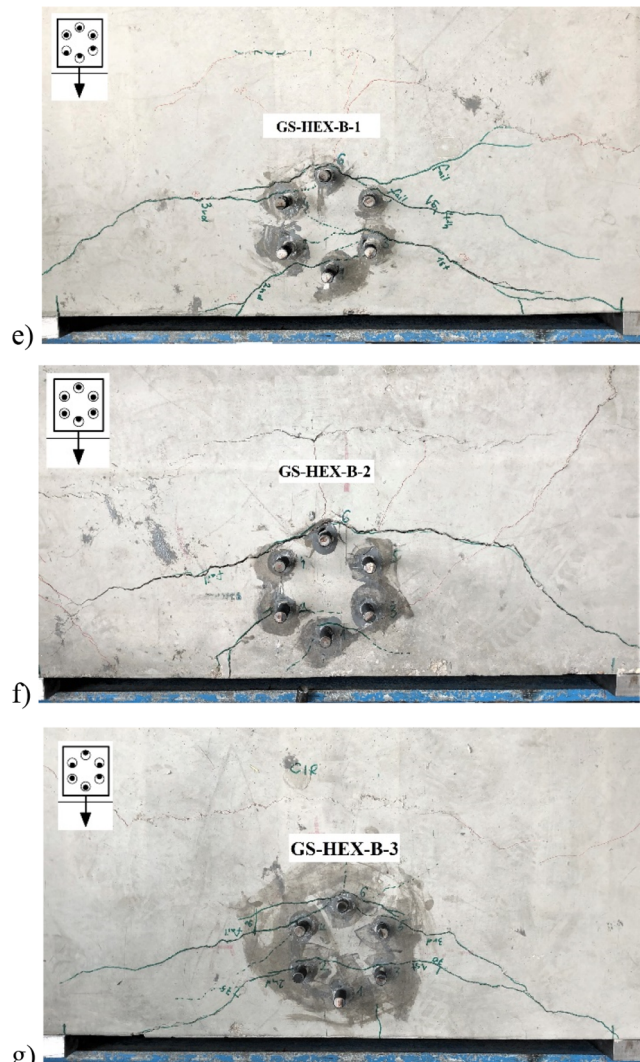


Fig. 17. (continued)

test 3. Due to this, the highest ultimate group load of the series could be reached. First, the anchor in the back row and anchor 3 in the second row were activated, followed by anchor 1 and finally by the third row. The displacement behaviour of the group is clearly shown by the observed crack pattern (Fig. 17g). No cracks have developed originating from the first and third rows. The first cracking occurred at 70 kN, originating from anchor 3, and the second at 75 kN from anchor 2. This is also indicated by the curve progression, however, only a slight loss of stiffness is visible at 75 kN applied load because a fast redistribution to anchors with higher stiffness was possible. The load-displacement curve shows that more anchors transferred the force in test 3 compared to test 1 and 2, which lead to a higher ultimate load and to higher stiffness and consequently, smaller displacement at failure.

Test series GS-HEX-A and GS-HEX-B showed that the failure crack always originates from the back anchor row and that independently from the hole clearance pattern, almost the same ultimate load could be reached in all three tests. However, the performance of the group is highly dependent on the displacement behaviour of the individual anchors of the group and on the actual hole clearance pattern. These will determine the influence of the cracking in the front row(s) (if any) on the group behaviour. Therefore, it is highly recommended to consider the load-displacement behaviour of the individual anchors of the group as well as the actual, or worst possible, hole clearance pattern when assessing or designing anchor groups.

#### 4. Summary and conclusions

The research work presented in this paper aimed to generate an experimental database on the concrete edge breakout failure of anchor groups loaded in shear perpendicular and towards the close edge. For this reason, anchor groups of rectangular ( $3 \times 1$ ,  $2 \times 1$ ) and non-rectangular (triangular, hexagonal) configurations were tested with random hole clearance pattern. To allow a comparison of the group performance with the behaviour of single anchors, reference tests were carried out with the edge distance of the corresponding anchor rows. Furthermore, the test program and the evaluation of the results aimed to provide the information required for the development of a relatively general analytical model for calculating the resistance of anchor groups in case of concrete edge breakout failure mode considering various anchor and hole clearance configurations, loading and boundary conditions.

The tests were evaluated in order to obtain information on (i) the group behaviour of anchorages, (ii) on the crack origination and propagation in case of anchor groups, (iii) on the influence of the displacement behaviour of single anchors on the behaviour of anchor groups and (iv) on the hole clearance pattern. A total of 56 shear loading tests were performed in non-cracked concrete on post installed (bonded) single anchors and anchor groups. The detailed evaluation of the test results such as load-displacement curves of the groups, load-displacement curves of single anchors, measurements on the hole clearance pattern and the investigation of the crack pattern supported the better understanding of the load-displacement behaviour of anchor groups.

The following major conclusions could be drawn:

- (1) For concrete edge failure the resistance increases with increasing edge distance.
- (2) The initial shear stiffness of the single anchors is independent of the edge distance provided all other parameters such as anchor type, size and embedment depth are the same.
- (3) The anchor group behaviour is highly dependent on the load-displacement behaviour of the individual anchors within the group. The failure load is relatively independent of the hole clearance pattern, whereas the group displacement and the activation of the individual anchors (and consequently the group stiffness) are influenced by the hole clearance pattern. The ultimate load of the groups was comparable with the reference single anchor series having the edge distance of the back anchor row. However, the stiffness of the group was higher and consequently, the displacement at failure was considerably lower.
- (4) For groups with two rows, in case of  $s_1/c_1 < 1$ , the cracking at the front anchor row was prevented due to the suppression of the cracking in the front row by the compression field, which is originating from the back anchor row. However, it is deemed that defining ratios to presume the group behaviour might only be expedient for certain configurations e.g.  $1 \times 2$ ,  $2 \times 1$  or  $2 \times 2$ . Although, the behaviour of the anchor groups - even in such configurations - depends on the displacement behaviour of the anchors, and it is assumed that the same configuration might result in different group resistance if the anchor type is changed.
- (5) Calculation of the group resistance assuming the failure crack initiation from the back anchor row (based on fib Bulletin 58) provides, in general, a good agreement with the experimental results. However, the information required for a safe design is not ensured without considering the displacement behaviour of the anchors and the hole clearance pattern. The investigated cases have shown that although the failure crack always originates from the back anchor row, the cracks developing at the front anchor row(s) might limit the design in serviceability limit state.
- (6) The single anchor tests carried out with a recess corresponding to the theoretical breakout body of an anchor in the front showed that

the presence of a pre-cast recess in front of the anchor has no significant influence on either the ultimate resistance or the stiffness of the anchors. This can be attributed to the fact that the concrete recess does not affect the breakout surface and the stress distribution in the load transfer area of the anchor is not disturbed. According to the authors, these tests are the first of these kinds to be performed and it is highly recommended to carry out further tests with different edge distance to recess dimension ratios to verify whether this conclusion remains valid even for other cases e.g., with the anchor installed rather close to the recess tip.

- (7) The single anchor tests (with  $c_1 = 240$  mm) carried out in pre-damaged specimen due to the failure of prior tests (with  $c_1 = 160$  mm) showed a large scatter in terms of the ultimate load as well as initial shear stiffness and displacement at failure. This is due to the significant influence of the pre-damage in the concrete on the "residual" resistance of the anchor. The investigation of the "residual capacity" of the back (tested) anchor does not give the required information about the possible performance of an anchor group having the same edge distance.
- (8) There is a significant influence of the hole clearance configuration on the anchor group behaviour. With a controlled hole clearance pattern, the most favourable pattern can be found and the best anchor group performance can be achieved. The hole clearance pattern can be controlled either by filling the annular gap with high-strength mortar before loading or by using slotted holes so that only particular anchors are resisting shear forces. Alternatively, the design can also be carried out for the most unfavourable hole clearance pattern. For that, all possible configurations must be analysed and the smallest value is decisive for the design. In the investigated cases, the random hole clearance pattern mostly influenced the displacement behaviour of the anchor group and only slightly the group resistance. This is an important aspect to consider since, however, the same ultimate load might be reached by the worse hole clearance pattern, the design might be limited due to excessive crack widths or displacements. Therefore, arbitrary anchor and hole clearance patterns are only possible to calculate accurately with displacement based approach considering the load-displacement behaviour of the individual anchors of an anchor group.
- (9) There is a need for a new model that can predict the concrete edge breakout resistance of anchor groups realistically, with sufficient accuracy. Ideally, the model should be able to consider the different geometric arrangement of the anchors, arbitrary hole clearance pattern, eccentric loading, cracked concrete, etc. Based on the test results presented in this paper, a new performance-based model for anchor groups loaded in shear close to the concrete edge is being developed and will be presented in a future paper.

#### CRediT authorship contribution statement

**Boglárka Bokor:** Conceptualization, Validation, Formal analysis, Investigation, Writing - original draft, Visualization. **Akanshu Sharma:** Conceptualization, Writing - review & editing, Supervision. **Jan Hofmann:** Supervision, Funding acquisition.

#### Declaration of Competing Interest

The authors declare that they have no known competing financial interests or personal relationships that could have appeared to influence the work reported in this paper.

#### Acknowledgements

The experimental investigations presented in this paper were financially supported by fischerwerke GmbH & Co. KG. The support

received from fischerwerke is greatly acknowledged. The opinions, findings, and conclusions or recommendations expressed in this publication are those of the authors and do not necessarily correspond with those of the sponsoring organisation.

#### Appendix A. Supplementary material

Supplementary data to this article can be found online at <https://doi.org/10.1016/j.engstruct.2020.111153>.

#### References

- [1] Elieghausen R, Mallée R, Silva JF. Anchorage in Concrete Construction. Berlin: Ernst & Sohn; 2006.
- [2] EN1992-4 Eurocode 2 Design of concrete structures - Part 4 Design of fastenings for use in concrete, European committee for standardization, Brussels, July 2018 EN1992-4:2018 (E).
- [3] Fédération Internationale du Béton (fib): Design of Anchorages in Concrete: Part I-V. Lausanne: International Federation for Structural Concrete (fib), 2011. (fib Bulletin 58).
- [4] ACI 318-14 Building Code Requirements for Structural Concrete and Commentary, ACI Committee 318, American Concrete Institute, 2014, ISBN: 97808070319303.
- [5] Fuchs W, Elieghausen R, Breen JE. Concrete Capacity Design (CCD) approach for fastening to concrete. ACI Struct J 1995;92:73–94.
- [6] Fuchs W. Tragverhalten von Befestigungen unter Querlast in ungerissenem Beton (Load-bearing behavior of fastenings under shear loading in uncracked concrete). Stuttgart, University of Stuttgart, Dissertation; 1990 (in German).
- [7] Hofmann J. Tragverhalten und Bemessung von Befestigungen unter beliebiger Querbelastung in ungerissenem Beton (Behaviour and design of anchorages under arbitrary shear load direction in uncracked concrete), Stuttgart, University of Stuttgart, Dissertation; 2005.
- [8] Schmid K. Tragverhalten und Bemessung von Befestigungen am Bauteilrand mit Rückhängebewehrung unter Querlasten rechtwinklig zum Rand (Behavior and design of fastenings at the edge with anchor reinforcement under shear loads towards the edge), Stuttgart, University of Stuttgart, Dissertation; 2010 (in German).
- [9] Unterweger A, Spyridis P, Mihala R, Bergmeister K. Shear loaded quadruple fastenings close to edge - Experimental and numerical analysis. Beton- Stahlbetonbau 2008;1013 Heft 11:741–7. <https://doi.org/10.1002/best.200800644>.
- [10] Tóth M, Bokor B, Sharma A. Anchorage in steel fiber reinforced concrete – concept, experimental evidence and design recommendations for concrete cone and concrete edge breakout failure modes. Eng Struct 2019;181:60–75. <https://doi.org/10.1016/j.engstruct.2018.12.007>.
- [11] A Unterweger Randahe Anker unter Querlast: mechanische Modellierung und Bemessung (Anchors close to edge under shear load). Vienna, Austria Universität für Bodenkultur, Dissertation; 2008 (In German).
- [12] Elieghausen R, Fuchs W. Load bearing behavior of anchor fastenings under shear, combined tension and shear or flexural loading. Betonwerk und Fertigteiltechnik 1988;2:48–56.
- [13] Fuchs W, Elieghausen R. Tragverhalten von Dübeln bei Querzug-, Schrägzug- und Biegebeanspruchung: Auswertung von Querzugversuchen an Einzel- und Mehrfachbefestigungen (Load-bearing behavior of anchorages under shear loading, combined shear and tension loading and bending: Analysis of shear tests with single anchors and anchor Groups). Stuttgart, University of Stuttgart, Institute of Construction Materials, 1986, Report No. 10/7 - 86/4, not published (in German).
- [14] Cruz RD. Effect of edge distance on stud groups loaded in shear and torsion. Stillwater Oklahoma State University School of Civil and Environmental Engineering; 1987. Master Thesis.
- [15] Wong TL, Donahey RC, Lloyd JP. Stud groups loaded in shear near a free edge. Stillwater: Oklahoma State University, Draft Paper, to be submitted to PCI in 1998.
- [16] Ruopp J, Kuhlmann U. Steel-to-Concrete joints with large anchor plates under shear loading. Steel Construct. 2017;10:115–24. <https://doi.org/10.1002/stco.201710015>.
- [17] Cook R, Klingner RE. Ductile multiple-anchor steel-to-concrete connections. J. Struct. Eng. ASCE 1992;118(6):1645–65.
- [18] Buia TT, Limani AW, Nana SA, Arrieta B, Roure T. Cast-in-place headed anchor groups under shear: Experimental and numerical modelling. Structures 2018;14:178–96. <https://doi.org/10.1016/j.istruc.2018.03.008>.
- [19] Epakcachi S, Esmaili O, Mirghaderi SR, Behbahani AAT. Behavior of adhesive bonded anchors under tension and shear loads. J Constr Steel Res 2015;114(2015):269–80. <https://doi.org/10.1016/j.jcsr.2015.07.022>.
- [20] Grosser P. Load-bearing behavior and design of anchorages subjected to shear and torsion loading in uncracked concrete. Germany: University of Stuttgart, Stuttgart; 2012. Ph.D Thesis.
- [21] Grosser P, Cook R. Load bearing behavior of anchor groups arranged perpendicular to the edge and loaded by shear towards the free edge. UF Structures Report 2009-1, University of Florida, USA; 2009.
- [22] Sharma A, Elieghausen R, Asmus J. Experimental investigation of concrete edge failure of multiple-row anchorages with supplementary reinforcement. Struct Concrete 2017;18:153–63. <https://doi.org/10.1002/suco.201600015>.
- [23] Sharma A, Elieghausen R, Asmus J, Bujnak J. Anchorages with supplementary reinforcement under tension, shear and interaction loads – experimental database, fib symposium 2019, Concrete – Innovations in materials, design and structures, May

- 27-29, 2019, Krakow, Poland.
- [24] EN 206:2014-07 Beton – Festlegung, Eigenschaften, Herstellung und Konformität; Deutsche Fassung EN 206:2013.
- [25] DIN EN 12390-1:2012-12 Prüfung von Festbeton – Teil 1: Form, Maße und andere Anforderungen für Probekörper und Formen; Deutsche Fassung EN 12390-1:2012.
- [26] ETA-10/0012 Europäische Technische Bewertung fischer Injektionssystem FIS EM, Deutsches Institut für Bautechnik, 19.03.2015.
- [27] Tian K, Ozbolt J, Sharma A, Hofmann J. Experimental study on concrete edge failure of single headed stud anchors after fire exposure. *Fire Saf J* 2018;96:176–88.  
<https://doi.org/10.1016/j.firesaf.2018.01.005>.
- [28] Anderson NS, Meinheit DF. PCI's headed stud design redefined. *Struct Mag* 2005;26–9.
- [29] Anderson NS. DF Meinheit A review of headed-stud design criteria in the sixth edition of the PCI design handbook. *PCI Journal* 2007;52(1):2–20.
- [30] Periškić G. Einzel- und Zweifachbefestigungen mit Verbunddübel senkrecht zum Rand unter Querlast zum Rand im ungerissenen Beton (Single anchors and groups with two anchors loaded in shear towards the edge in uncracked concrete), Report No. E06/01-E01301/1, University of Stuttgart, Stuttgart; 2006 (in German).